Renato Brito Moreira dos Santos

Licenciado em Química

Development of Electrospun Ion Jelly Fibers® for Drug Delivery

Dissertação para obtenção do Grau de Mestre em Biotecnologia

Orientador: Doutor Pedro Miguel Vidinha Gomes
Co-orientador: Prof. Doutor João Paulo Borges

Júri:

Presidente: Prof. Doutora Ana Cecília Afonso Roque
Arguente(s): Doutor Nuno Miguel Torres Lourenço
Vogal(ais): Doutor Pedro Miguel Vidinha Gomes

FACULDADE DE CIÊNCIAS E TECNOLOGIA
UNIVERSIDADE NOVA DE LISBOA

Dezembro 2011

“Copyright”

Development of Electrospun Ion Jelly® fibers for Drug Delivery

- Renato Brito Moreira dos Santos
- Faculdade de Ciências e Tecnologia
- Universidade Nova de Lisboa

A Faculdade de Ciências e Tecnologia e a Universidade Nova de Lisboa têm o direito, perpétuo e sem limites geográficos, de arquivar e publicar esta dissertação através de exemplares impressos reproduzidos em papel ou de forma digital, ou por qualquer outro meio conhecido ou que venha a ser inventado, e de a divulgar através de repositórios científicos e de admitir a sua cópia e distribuição com objectivos educacionais ou de investigação, não comerciais, desde que seja dado crédito ao autor e editor.

ACKNOWLEDGMENTS

First and foremost I would like to thank my supervisors, Dr. Pedro Vidinha and Prof. Dr. João Paulo Borges for giving me the opportunity to do my master thesis in their groups. I'm extremely grateful for their support and advices during my work. Thank you.

I am also grateful to Isabel Sá-Nogueira for letting me work in her laboratory and for all her advices.

I would like to thank all my "Lab mates", which are spread across 3 laboratories. Very special thanks to Tânia Carvalho, for all her help since the very first day, when she taught me how to make Ion Jelly! I would also like to say thank you to Angelo Rocha for providing me all the ionic liquids and polymers.

I would like to thank Dr. Ana Nunes and Dr. Catarina Duarte for the toxicological results.

Thank you to all my family, for their love and support. Thank you for giving me power and confidence to overcome all my challenges and problems. Thank you for not giving up on me!

Thank you to all my friends. I'll always be grateful to Andreia Melo, Ana Raquel, Bruno Martins, Susana Reis, Sara Matias, João Alves, Joana Sequeira and Liliana Rodrigues for their unconditional support. Without you I just could not be what and where I am now. Thank you for all the good laughs, advices and, specially, for taking care of me!

At last, but certainly not the least: Thank you, David Sher.

Resumo

Este trabalho centra-se no desenvolvimento de um sistema de libertação controlada de fármacos baseado em fibras de Ion Jelly (IJ). O IJ é um material versátil que resulta da combinação da gelatina com um líquido iónico (IL).

Vários ILs baseados em colina e princípios activos farmacêuticos (API) foram utilizados para formar IJs. Os ILs utilizados foram: acetato de colina ([Ch][Ac]), mandelato de colina ([Ch][Ma]), tiglato de colina ([Ch][Ti]) e ibuprofenato de colina ([Ch][Ib]).

As fibras de IJ aqui relatadas foram produzidas através da técnica de electrofiação, permitindo a obtenção de fibras com diâmetros reduzidos e elevada área superficial. Esta abordagem teve como objectivo evitar a baixa taxa de difusão característica dos ILs, resultante da elevada viscosidade.

O impacto dos parâmetros da electrofiação na produção de fibras foi avaliado. Verificou-se que a concentração de IL na solução era o parâmetro com mais impacto na obtenção e morfologia das fibras.

A avaliação morfológica das fibras de IJ foi realizada recorrendo às técnicas de microscopia óptica e microscopia electrónica de varrimento. Observou-se que as soluções de IJ-[Ch][Ib] produziram fibras com diâmetros ligeiramente inferiores às restantes, especialmente quando comparadas com as soluções de IJ-[Ch][Ti].

As propriedades antimicrobianas do ácido mandélico, [Ch][Ma] e fibras de IJ-[Ch][Ma], foram testadas em *Escherichia coli* K-12 e *Bacillus subtilis* T168. Os resultados demonstram que a actividade antimicrobiana de [Ch][Ma] foi bastante melhorada com a encapsulação em fibras de IJ. Para além deste resultado, os ensaios de toxicidade revelaram que só o IL-[Ch][Ib] se apresentou como tóxico, estando em concordância com a toxicidade apresentada pela forma cristalina de ibuprofeno.

Os resultados dos ensaios de tracção evidenciam o impacto da água no comportamento mecânico e elasticidade do IJ.

Por último, foi testada a electrofiação de IJ usando o DNA e N,N-Dimetilquitosano como polímeros. Contudo, não foi possível a obtenção de fibras.

Palavras-chave: Líquidos iónicos, Ion jelly, electrofiação, princípios activos farmacêuticos, libertação controlada.

Abstract

The aim of this work was the development of a drug delivery system based on Ion Jelly fibers. Ion Jelly (IJ) is a highly versatile polymeric material and is the result from the combination of gelatin and an ionic liquid (IL).

For that purpose, different IJs were created using ILs based on choline and active pharmaceutical ingredients. The ILs used were choline acetate ([Ch][Ac]), choline mandelate ([Ch][Ma]), choline tiglate ([Ch][Ti]) and choline ibuprofenate ([Ch][Ib]).

IJ fibers for drug delivery systems were produced through electrospinning, owing to its ability of producing polymeric fibers with reduced diameters and high surface area. The aim of this approach was to overcome the low diffusion rate that the above ILs exhibit due to their high viscosity.

The impacts of electrospinning parameters on fiber production were evaluated. We verified that the most important parameter to achieve defect-free and thin IJ fibers was IL concentration.

Morphological studies of IJ electrospun fibers were performed through optical microscopy and scanning electron microscopy. It was observed that IJ - [Ch][Ib] yielded slightly thinner fibers when compared with IJ-[Ch][Ti] fibers.

The results from antibacterial tests using mandelic acid, [Ch][Ma] and IJ-[Ch][Ma] fibers as antibacterial agents against *Escherichia coli* K-12 and *Bacillus subtilis* T-168 prove that [Ch][Ma] encapsulation in IJ electrospun fibers greatly increased the IL properties. In addition, toxicological data suggest that the ILs studied were not toxic with the exception of [Ch][Ib] which shows a similar toxicity to crystalline ibuprofene.

In addition, tensile tests suggest that water content has an important impact on both IJ mechanic behavior and elasticity.

Additionally, we also evaluated the fabrication of IJ fibers using other polymers beyond gelatin, namely DNA and N,N-Dimethylchitosan. Nevertheless, no fibers were obtained.

Keywords: Ionic liquids, Ion Jelly, electrospinning, active pharmaceutical ingredients, drug delivery.

Index of Contents

Index of Images

Index of Tables

List of Abbreviations

Compounds and ions

$[Ace]^-$ - Acesulfamate anion

AHA - Alpha hydroxy acid

$[A]^-$ - Anion

$[BA]^+$- Benzalkonium cation

$[Ben]^-$ - Benzoate anion

$[bmim]^+$ – 1-butyl-3-methylimidazolium cation

[bmim][Cl] - 1-butyl-3-methylimidazolium chloride

[bmim][dca] - 1-butyl-3-methylimidazolium dicyanamide

$[bmim][PF_6]$ - 1-butyl-3-methylimidazolium hexaflouorophosphate

$[bmim][BF_4]$ - 1-butyl-3-methylimidazolium tetrafluoroborate

$[C_2OHmim][BF_4]$ - 1-(2-hydroxyethyl)-3-methyl-imidazolium tetrafluoroborate

[Ch][Ac] – Choline Acetate

[Ch][Ib] – Choline ibuprofenate

[Ch][Ma] – Choline Mandelate

[Ch][Ti] – Choline Tiglate

CsCl – Cesium chloride

$[DDA]^+$- Didecyldimethylammonium cation

DNA – Deoxyribonucleic acid

$[DOM]^+$- Domiphen cation

[emim][dca] - 1-ethyl-3-methylimidazolium dicyanamide

$[emim][BF_4]$ - 1-ethyl-3-methylimidazolium tetrafluoroborate

KCl – Potasium Chloride

NaCl – Sodium Chloride

$[omim][BF_4]$ – 1-octyl-3-methylimidazolium tetrafluoroborate

PCL – Polycaprolactone

PEO – Polyethylene glycol

PLA – Polylactic acid

PLGA – Poly(lactic-*co*-glycolic acid)

PVA – Polyvinyl alcohol

$[Sac]^-$ - Saccharinate anion

siRNA – Small interfering RNA

$[TBA]^+$ - Tetrabutylammonium cation

$[Tr]^-$ - Triazole anion

Units and measures

% w/v – Weight / volume percentage

% v/v - Volume / volume percentage

σ' – Conductivity

σ_b – Stress at break

ε_b – Strain at break

η – Dynamic viscosity

ºC – Celsius

cm - Centimeter

cP – Centipoise

E – Young's modulus

G – Shear modulus

g – Gram

g / mol – Gram per mol

kV – Kilo volt

keV – Kilo electronvolt

MPa – Mega Pascal

µL - Microliter

µm – Micrometer

µM – Micromolar

mg – Milligram

mm – Millimeter

mL / h – milliliter per hour

min – Minute

M_w – Molecular weight

nm – Nanometer

Pa - Pascal

S/cm – Siemens per centimeter

T_g – Glass transition temperature

T_m – Melting point

M_w – Molecular weight

V – Volt

W/g – Watt per gram

Other abbreviations

AIDS - acquired immunodeficiency syndrome

API – active pharmaceutical ingredient

B. subtilis – *Bacillus subtilis* T168

DRS – Dielectric relaxation spectroscopy

DSC – Differential scanning calorimetry

EC50 – Half maximal effective concentration

E. coli – *Escherichia coli* K-12

HIV - Human immunodeficiency virus

IBET – Instituto de Biologia Experimental e Tecnológica

IJ – Ion Jelly®

IL – Ionic liquid

KF – Karl Fischer

LB – Lysogeny broth

MRSA – Methicillin resistant *Staphylococcus aureus*

OM – Optical Microscope/Microscopy

SEM – Scanning electron microscopy

UV/Vis – Ultraviolet / Visible

VOC – Volatile organic compound

1 INTRODUCTION

1.1 Ionic Liquids

Ionic Liquids (ILs) are salts with a melting point below 100 ˚C [1]. They are exclusively composed by ions and during the last decade they have been considered a "hot topic" in science not only due to their huge range of applications but also because most of them are environmental friendly compounds.

Although they were known for over a century, only in 1992 they have started gathering relevant attention when air and water stable ILs like [emim][BF_4] were reported [2].

Since then there has been a continuous growing interest in these liquids, owing to their unusual properties such as low vapor pressure, low melting point, chemical and thermal stability, liquid range, relatively high conductivity, low flammability, wide electrochemical window, relatively low viscosity, solvation versatility or tunable properties. There is also a huge potential for their development and there is a growing interest to synthesize novel ILs or to test different combinations of ions in order to, not only scope the ILs and their applications, but also to enhance their remarkable properties [1].

The properties of ILs are a result of the combining ions. There is a large number of ions available and their possible combinations are virtually limitless. For this reason ILs have been described as "designer solvents", as their properties can be targeted or adjusted to a specific function or task [3].

1.1.1 Properties

The unusual features presented by a given IL are a result of the structure of their constituent ions and consequent interactions [4]. Unlike crystalline salts, ILs do not possess the ability to form a truly organized crystalline lattice, because they are usually composed by larger or unsymmetrical ions. It is known that an increase of the ion's size leads to a decrease of its surface charge density, resulting in weaker electrostatic forces between ions, and it can be exemplified through the melting point of simple inorganic salts such as NaCl (T_m= 803˚C), KCl (T_m= 772˚C) or CsCl (T_m= 646˚C) [5]. Krossing *et* al. found that the fusion's Gibbs free energies for fourteen ILs at room temperature (25 ˚C) were all negative, demonstrating that the liquid state is thermodynamically favorable under those conditions. The main reasons associated with the results are the larger size, weakly coordinating nature and conformational flexibility of the ions involved [6].

The most common ions used to synthesize ILs are depicted in **Figure 1.1**. The cations used are usually substituted derivates of imidazolium, pyridinium, pyrrolidinium, tetra-alkyl ammonium and tetra-alkyl phosphonium ions. The most common anions used are Cl^-,PF_6^- and BF_4^-. Nevertheless, these ions are being substituted by other more environmentally friendly ones such as alkylsuphates, lactate, acetate, hydrogencarbonate, acesulfamate and saccharinate anions or other benign cations like cholinium [7-11].

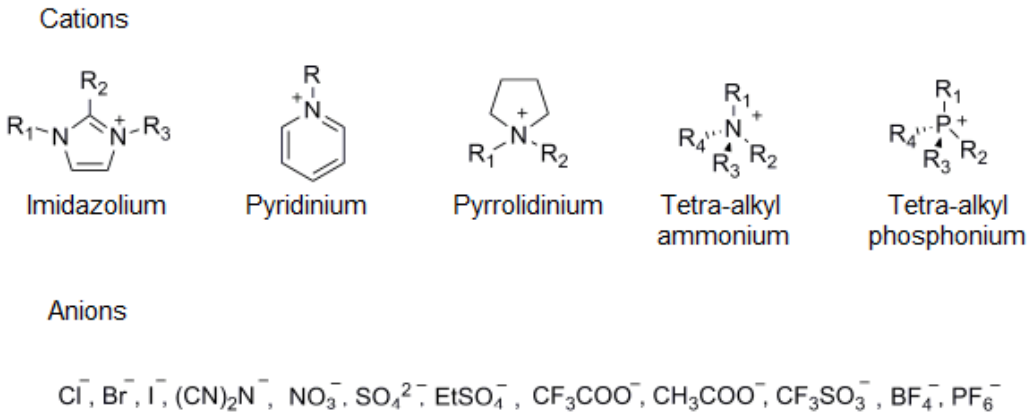

Figure 1.1 – Most commonly used ions in IL.

The functionalization and the length of alkyl chain have an important impact on IL properties, For instance, Erdmenger *et* al. analyzed the influence of side linear and branched alkyl chains on derivates of 3-methylimidazolium ions, concluding that not only the water uptake decreases as long as the length of branched and linear alkyl chain increases, but also the water uptake is higher for branched alkyl chains when compared with linear alkyl chains due to their low self-assembly capacity [12]. Solubility of 1- alkyl-3-methylimidazolium ions were analyzed by Holbrey and Seddon [13]. These authors verified that ILs with a side alkyl chain lower than six carbons were miscible with water at 25 ºC. On the other hand, their miscibility was dramatically affected when the alkyl chain had more than six carbons.

Moreover, alkyl chain length also has effect on ILs' melting point. Holbrey and Seddon analyzed the thermal stability and melting points of 1-alkyl-3-methylimidazolium tetrafluoroborates and hexafluorophosphates. They found that an increase on the alkyl chains' length usually led to higher melting points due to stronger van der Waals interactions[13, 14], and lowers the liquid density [3, 15, 16].

Nevertheless, ILs properties are not exclusively dependent on cationic structure. Huddleston *et* al. investigated how water miscibility of 3-methylimidazolium IL was affected by the correspondent anion. The ionic liquids $[C_n mim][PF_6]$ (n = 4, 6, or 8) were not miscible with

water whereas [$C_n$mim]Cl (n = 4, 6, or 8) were, showing that the anion has also a critical influence on the IL properties [15].

Among ILs' properties, low vapor pressure is one of the most appreciated features and the main reason behind the claims of environmental friendliness. It was once believed that IL did not evaporate and had no vapor pressure at all [14]. Nowadays it is known that ILs have a low vapor pressure and that they can even be distilled at high temperature (above 300ºC) and reduced pressure without thermal degradation [17, 18], showing also its thermal stability. The remarkably low flammability and volatility of IL – 10^{-11} Pa for [bmim][PF_6] at 25ºC [19] – are considered an advantage over toxic, flammable volatile organic compounds (VOC's) that can be dangerous for human health and environment. For those reasons and because ILs solvation properties could be easily modified, ILs have been considered an attractive media for safe and green synthesis [20]. From an engineering standpoint ILs' low vapor pressure can represent a big operational advantage over VOC's because chemical separations based on distillation can be easily performed with these liquids, avoiding solvent distillation and azeotrope formation [3].

One of the drawbacks attributed to ILs is their high viscosities. In fact, viscosity has a negative impact on mass transfer and diffusion rates. Compared to other solvents, ILs have higher - sometimes much higher – viscosities than most used solvents, being more comparable with a typical oil [15]. The lower range of viscosity values for IL is around 20 cP (water viscosity is 1 cP at 20ºC). MacFarlane *et* al. reported that viscosity for [emim][dca] at 25ºC is 21 cP [21]. For practical applications, high viscosities can result in significant power requirements if mixing is needed [16]. Again, like other properties, viscosity can be modified by changing the combining ions or the aforementioned alkyl chain's length.

Table 1.1 – Dynamic viscosities (η) of various $[bmim]^+$ salts at 20ºC [3].

	Anion $[A]^-$	η [cP]
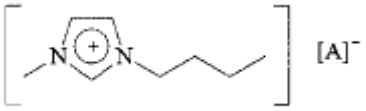	$CF_3SO_3^-$	90
	n-$C_4F_9SO_3^-$	373
	CF_3COO^-	73
	n-$C_3F_7COO^-$	182
	$(CF_3SO_2)_2N^-$	52

Table 1.1 demonstrates that viscosity is positively correlated with the intensity of Van der Waals interactions and hydrogen bonds. The van der Waals effect is revealed by the difference of viscosity values of [bmim][$CF_3SO_3^-$] and [bmim][CF_3COO^-] with [bmim] [*n*-$C_4F_9SO_3$] and [bmim][*n*-$C_3F_7COO^-$], respectively. The lower viscosity of [bmim][$(CF_3SO_2)_2N^-$] compared to [bmim][$CF_3SO_3^-$] is an evidence of the hydrogen bond's influence in viscosity. The viscosity value is lower even with the increase of van der Waals interactions.

Since ILs are composed solely by ions their electrochemical properties aroused a great interest. Some ILs have high values of conductivity, like [bmim][BF_4] ($3.4x10^{-2}$ S/cm at 25ºC)[22]. Higher conductivities around 10^{-1} S/cm at room temperature were also reported [23, 24]. Conductivity values obtained with alkylimidazolium cations revealed that conductivity is generally proportional to the inverse of viscosity and the ions' mobility is of vital importance [22, 24, 25].

Another important and appreciated feature in ILs is the wide electrochemical stability. In fact, the electrochemical window of a given solvent is an important parameter for electrochemical applications, requiring that the solvent supports the voltage of operation [26]. Some ILs can have electrochemical windows of 5 and 6 V of range, depending on work conditions. Suárez *et* al. verified that [bmim][BF_4] has a electrochemical window of 6,1 V and 4,6 V using tungsten and platinum as working electrodes, respectively, against the platinum reference electrode [27]. In the same study [bmim][PF_6] was found to have an electrochemical window of 5,7 V using both platinum as working and reference electrodes. This electrochemical stability is an important advantage and is one of the reasons for the growing interest in ILs for electrochemical applications.

1.1.2 Applications

The structural flexibility, virtually infinite combinations of ions results in a range of properties that earn IL an unusually variety of possible applications.

ILs liquid nature, broad liquid range, chemical stability and low vapor pressure were the features behind their first use as alternative "designer solvents" and new reaction media towards a "greener chemistry". Up to this day, after years of research, there is a countless number of examples about the advantages of these liquids as solvents [3, 16, 20, 28, 29]. One of the most striking examples of the tunable properties and solvation strength of ILs is their capability to dissolve polymers such as cellulose [30] or chitin [31]. Cellulose can be dissolved without derivatization in high concentrations - 25 % w/v in [bmim][Cl]. This cannot be achieved with conventional inorganic or organic solvents [30]. Catalysis and biocatalysis are other areas where ILs have been tested and used as solvents, providing an even greener solution for catalytic transformations [3, 29, 30, 32, 33].

As an electrically charged fluid, it is not surprising that ILs have been exhaustively studied for electrochemical applications such as: electrolytes for fuel cells, lithium rechargeable batteries and electrochemical capacitors [34]. Most electrolytes used for lithium rechargeable batteries are composed of lithium salts dissolved in a mixture of volatile organic solvents [35].

The replacement of these solvents with ILs with high ionic conductivities, low vapor pressures and low flammabilities in order to produce safer electrolytes is of major interest [34]. Another approach is to incorporate an IL into a solid-state polymer electrolyte, like Shin *et* al. demonstrated with the example of polymerized PEO with boosted conductivity after IL's addition [36]. Souza *et* al. verified that ILs are an excellent alternative for alkaline hydrogen and air operated fuel cells, achieving an overall energetic efficiency around 67% using [bmim][BF_4] as electrolyte at room temperature and atmospheric pressure [37].

Polymeric conducting materials can also be obtained combining ILs with biopolymers. In fact, this is a recent area for the application of ILs [38, 39]. One of the best examples was reported by Vidinha *et* al. who obtained a polymeric conducting material combining gelatin and ILs, creating an Ion Jelly (IJ) that combines the conductible nature of ILs with the mechanical versatility of a biodegradable polymer. These features can allow the development of smart and tailor-made electrochemical devices such as batteries, fuel cells, electrochromic windows or photovoltaic cells [40].

IJ has an interesting versatility which is derived of ILs' tunable properties. IJ primary use has been as a polymeric conductor material, exploiting ILs and resulting IJ high conductivities [40]. IJ is also being studied as a platform for enzyme-entrapment for bionsensors development [41]. The entrapment of enzymes in the polymeric matrix decreased their activity compared to the free enzyme. However, enzymes' stability was dramatically improved, including protection from deactivation from high concentrations of hydrogen peroxide. Enzyme entrapment in a polymer support opens up the possibility of creating smart test devices like the glucose detection paper strip developed by Lourenço et al [41].

Because of their versatility, ILs are currently being studied as alternative chemicals in a broad range of different areas like: nanotechnology [42], tribology (for the development of lubricants based in highly viscous ILs) [43], gas handling [44], analytical chemistry [45], magnetic fluids [46], propellants [47], optical devices [48], separation membranes [49] or energy fluids [50]. The main development areas are illustrated in **Figure 1.2**.

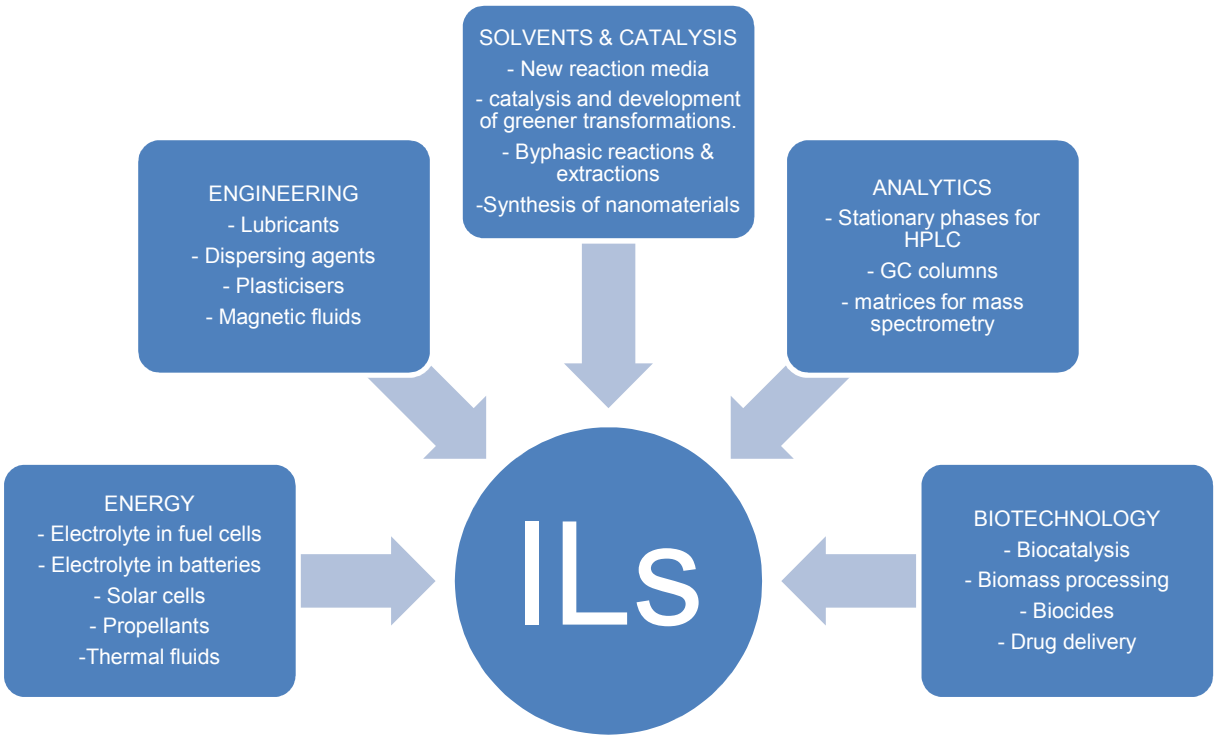

Figure 1.2 - Possible application areas for ILs.

For the last years, ILs have aroused a great interest and countless studies in the academic world. Despite the limited number of examples, ILs have already made their way into industry and commercial applications, in particular gas enterprises like Air Products and Linde. Air Products use ILs to carry hazardous gases like phosphine and arsine and Linde makes use of ILs to compress gases like hydrogen in pumping stations [51, 52].

The most well-known commercial application of ILs is the BASIL™ process developed by BASF AG in 2002, used in the production of alkoxyphenylphosphines [11, 53]. The abbreviation stands for "Biphasic Acid Scavenging utilizing Ionic Liquids". In the previous process, triethylamine was used to scavenge the acid formed, converting the reaction mixture in a suspension that was difficult to handle and mix because of the triethylammonium chloride that was formed. The new process replaces triethylamine with 1-methylimidazole leading to the formation of 1-methylimidazolium chloride, which creates a distinct phase in the reactor. The IL's recycling easiness and the immiscibility of the distinct phases improved the process yield from 50% to 98%, representing a huge amount of saving costs and increase of productivity [11, 53].

1.2 Ionic Liquids: active pharmaceutical ingredients

1.2.1 Toxicity and antimicrobial properties

ILs are usually grouped into three distinct generations, based on their properties [54]. The first generation of ILs includes those which have tunable physical properties like low vapor pressure or broad liquid range. The second generation group includes those that combine physical with chemical properties, allowing specific applications like those indicated in the aforementioned "Applications" topic.

The third generation of ILs includes those which combine a physical or chemical property with a biological one. ILs are considered "green chemicals" but there has been an increasing need to evaluate the real environmental problems of these liquids. Given that ILs are candidates for use in consumer goods, major concerns about their toxicity and biocompatibility have emerged [55]. In fact, some studies, most of them centered on imidazolium based ILs, suggest that some ILs can be as toxic, or even more toxic, than ordinary organic solvents [56]. Toxicity is a biological property. Like the other properties present in ILs, toxicity can be also tuned and modified. Matzke *et* al. verified also that imidazolium based ILs' toxicity is positively correlated with alkyl's chain length, demonstrating that some ILs, like [bmim][BF_4] or [omim][BF_4], have higher toxicities than acetone or acetonitrile [57].

1.2.2 Choline-based IL

Taking into account the high toxicity of several ILs, there has been a growing interest towards the development of less hazardous ILs. As mentioned before, several biocompatible ions have been used for IL development, such as alkylsuphates, lactate, acetate, hydrogencarbonate, acesulfamate and saccharinate anions [7-11].

The most usual strategy to modify ILs' properties (toxicity included) is through changing the anion or its substituents. However, attempts are being made in order to explore the possibilities that cation modifications can bring. Regarding toxicity, cholinium cation has been successfully used in the synthesis of environmental friendly and biocompatible ILs. Choline is an essential nutrient and a precursor of the neurotransmitter acetylcholine [58].

Choline-based or choline-like ILs have been used in catalysis for carbonyl protection [59]. Choline-based ILs can also be used as cross-linking agents for biomaterials [60], protein and nanoparticles stabilizers [61, 62] or sample preparation for microscopy observation [63].

The modification of cholinium substituent groups can also lead to the development of lipophilical antibacterial ILs. As written in section **1.2.4,** antibacterial ILs are usually composed by quaternary ammonium cations. This two factors combined opened up the possibility of developing environmental friendlier ILs based on cholinium cation with enhanced biocompatibility. Pernak *et* al. synthetized and evaluated the antibacterial properties of a vast range of choline-based ILs, demonstrating the potential of cholinium cation to develop a whole new group of antibacterial agents [64, 65].

1.2.3 Polymorphism and drug failure

Nowadays the pharmaceutical industry's active pharmaceutical ingredients (API) are essentially commercialized in the solidified crystalline form. This preference is related with thermal stability, purity, ease of handling and manufacture [66]. Despite this preference, pharmaceutical companies spend an enormous amount of money and time to guarantee that a given crystalline API matches the quality standards required to be commercialized. The reason behind all this effort is polymorphism.

Polymorphism is defined as a property of a substance to exist in more than one crystal structure [67]. Even though crystalline polymorphs have the same chemical composition, they differ in their physical-chemical properties because their crystalline lattice and structure are distinct. This difference in the crystalline lattice has consequences in diverse properties such as, density, chemical stability, solubility, rate of dissolution, melting point or interactions with biological systems [67]. Pseudopolymorphism is associated with a crystal lattice formed with molecules of solvent and the solute [68]. (Pseudo)polymorphism poses a great challenge to pharmaceutical industry not only because companies have to deal with polymorphs as soon as the API is being developed and produced (in order to find the best and most stable one), but also because polymorph behavior can be quite unpredictable.

A paradigmatic example of the problems aroused from polymorphism is the case of anti-HIV drug ritonavir, introduced by Abbot Laboratories in 1996 as Norvir. The only polymorph developed and commercialized then, known as form I, had bioavailability problems in the solid state if given by oral route. Because of that, Norvir was commercialized in a liquid oral form or capsules filled with a mixture of water/ethanol solution. Norvir, being commercialized in a liquid form, didn't require polymorph control [69]. After two years, however, some lots had serious problems with dissolution and bioavailability. After the evaluation of these lots, it was concluded that a new polymorph, thermodynamically-stable form II, had appeared and precipitated due to its decreased solubility, revealing that form I was the kinetic product [69]. The drug, in order to continue in the market, had to be reformulated, including the manufacture procedure, as the

new polymorph was more stable and prevailed for some time as the dominant form [69]. These factors combined not only to limit inventory and seriously threatened the supply of this life saving treatment for AIDS, but also forced Abbot Laboratories to spend more money and time to redevelop the drug.

Other examples of drugs that need careful control of polymorphism, due to water solubility problems, are: Torsemide, a diuretic; carbamazepine, an anticonvulsant; warfarin sodium, an anticoagulant; or cefuroxime axetil, which is a broad-spectrum cephalosporin antibiotic [70].

Most commercialized drugs are orally administrated. Polymorphism and other features like, lipophilicity, drug's ability to be dissolved by natural surfactants, ingested food and drug's own pKa values are crucial for achieving good bioavailability and therapeutic effect [71]. One of the main reasons for drug development failure, beyond polymorphism, is that *in vitro* data is, usually, not useful to predict the drug's therapeutic results *in vivo*. This means that it is difficult to replicate the gastro-intestinal environment and simulate accurately an orally administrated drug's path and transformations [71].

With this in mind, it may be useful to develop and study new ways to formulate APIs with the objective to overcome the aforementioned issues. ILs, being in liquid form and having tunable properties, are now considered attractive by pharmaceutical industry not only as solvents, but also as chemicals to eliminate the problems addressed in this topic [54, 72]. Hough *et* al. noticed that some ILs forming ions resembled API or API precursors. Both were large, asymmetric and had the possibility to delocalize charges [54]. Therefore, obtaining ILs with API ions should not be a difficult task.

1.2.4 ILs as active pharmaceutical ingredients

The potential toxicity of ILs triggered the interest to study and confirm their potential as antimicrobial agents [64, 65, 73-83]. The mechanism of action is thought to be via membrane interaction [83] – a bigger alkyl chain is more lipophilic and interacts better with the cells' membrane. Bernot *et* al. suggested that membrane-bound proteins are disrupted by ILs in the same way as cationic surfactants do [84]. Inhibition of pure enzyme acetylcholinesterase by imidazolium and pyridinium based ILs (with EC50 concentrations as low as 13 μM) has also been reported and suggested as a way of mechanism for IL toxicity [85]. Actually, most of the ILs found to have antimicrobial properties are imidazolium, pyridinium and ammonium-based. **Figure 1.3,** depicted in next page, illustrates some examples.

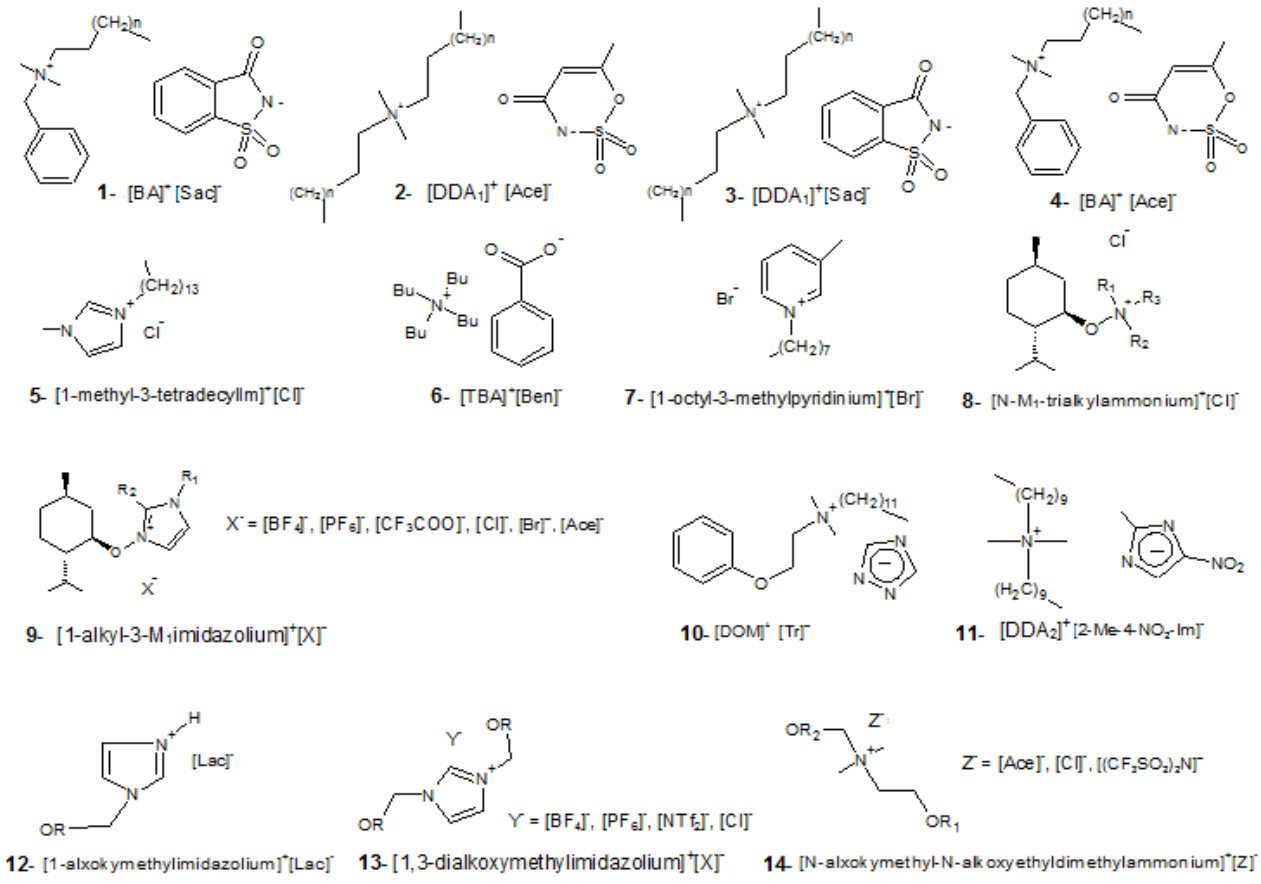

Figure 1.3 – Examples of ILs with antibacterial properties.

All the examples shown in **Figure 1.3** are ILs with nitrogen containing cations. All the examples have in common the fact of having long alkyl chains, which is an important factor to their antimicrobial properties. Some of them are composed of quaternary ammonium cations, which are well known for their broad range of applications, especially as bactericides and desinfectants [73]. Noteworthy are the ILs **1** to **4**, demonstrating the concept of pairing a biological activity of the cation with a distinct biological function, provided by non-nutritive sweeteners saccharinate and acesulfamate anions [73]. This, for example, can lead to develop products that can be orally administrated with a pleasant taste. Examples **8** and **9** demonstrate the synthesis of new chiral ILs. Beyond their antimicrobial properties, these ILs can be used as reaction media for chiral synthesis [77, 78]. Carson *et* al. reported that 1-alkyl-3-methylimidazolium ions revealed excellent antimicrobial properties against a variety of biofilms, which are a clinical problem, including multidrug resistant organisms like methicillin resistant *Staphylococcus aureus* (MRSA) and a large variety of other pathogens [75]. MRSA is, for example, one common pathogen causing infectious outbreaks in hospitals or intensive-care units constituting a problem to public health [86, 87]. These examples showed above reveal that ILs have an enormous development potential in the fields of antiseptics, desinfectants and anti-bacterial agents.

The biological properties of ILs are not purely centered on their antimicrobial properties. Kumar and Malhorta demonstrated for the first time the anticancer properties of ILs [88]. The ILs, depicted in **Figure 1.4**, are based in ammonium and phosphonium ions, being the latter case more effective inhibiting tumorous-cells growth. Not surprisingly, the results also revealed that efficacy is correlated with ILs' alkyl chains length [88].

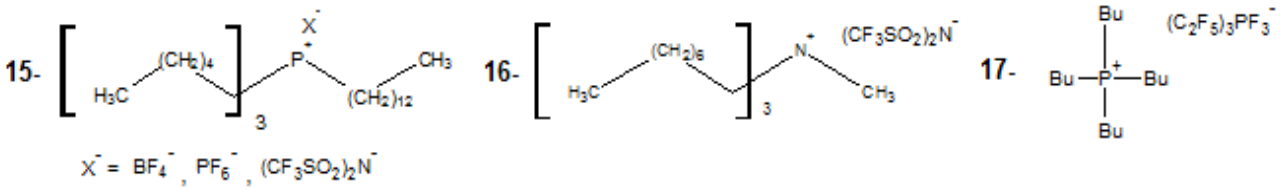

Figure 1.4 – Examples of ILs with anticancer properties [88].

The vast possibilities of ions' combinations may result in salts with new and unique properties that wouldn't be explored if crystallization was a decisive factor [72]. One of the best examples of unique properties given by the ions' synergic effect is the example of Lidocaine Docusate (structure **19** on **Figure 1.5**) [54]. Lidocaine hydrochloride, used as local anesthetic, was combined with sodium docusate, an emollient, to form a hydrophobic IL that, not only has an improved lipophilicity, but can also remain longer times on the skin [54]. Noteworthy is the increased membrane permeability, which improved efficiency and therapeutic effect, but also a modification of the drugs mechanism of action, more consistent with a slow drug release pattern [54]. In the same study, it was also reported the synthesis of other ILs including the ibruprofenate anion, in a perspective of developing ILs where the primal biological function is anion-related instead of the more common "cation-approach" [54], and also an IL with the ranitidine cation. Ranitidine hydrochloride, GlaxoSmithKline's Zantac, is an anti-ulcer that caused major litigations based on polymorphs and purity [89].

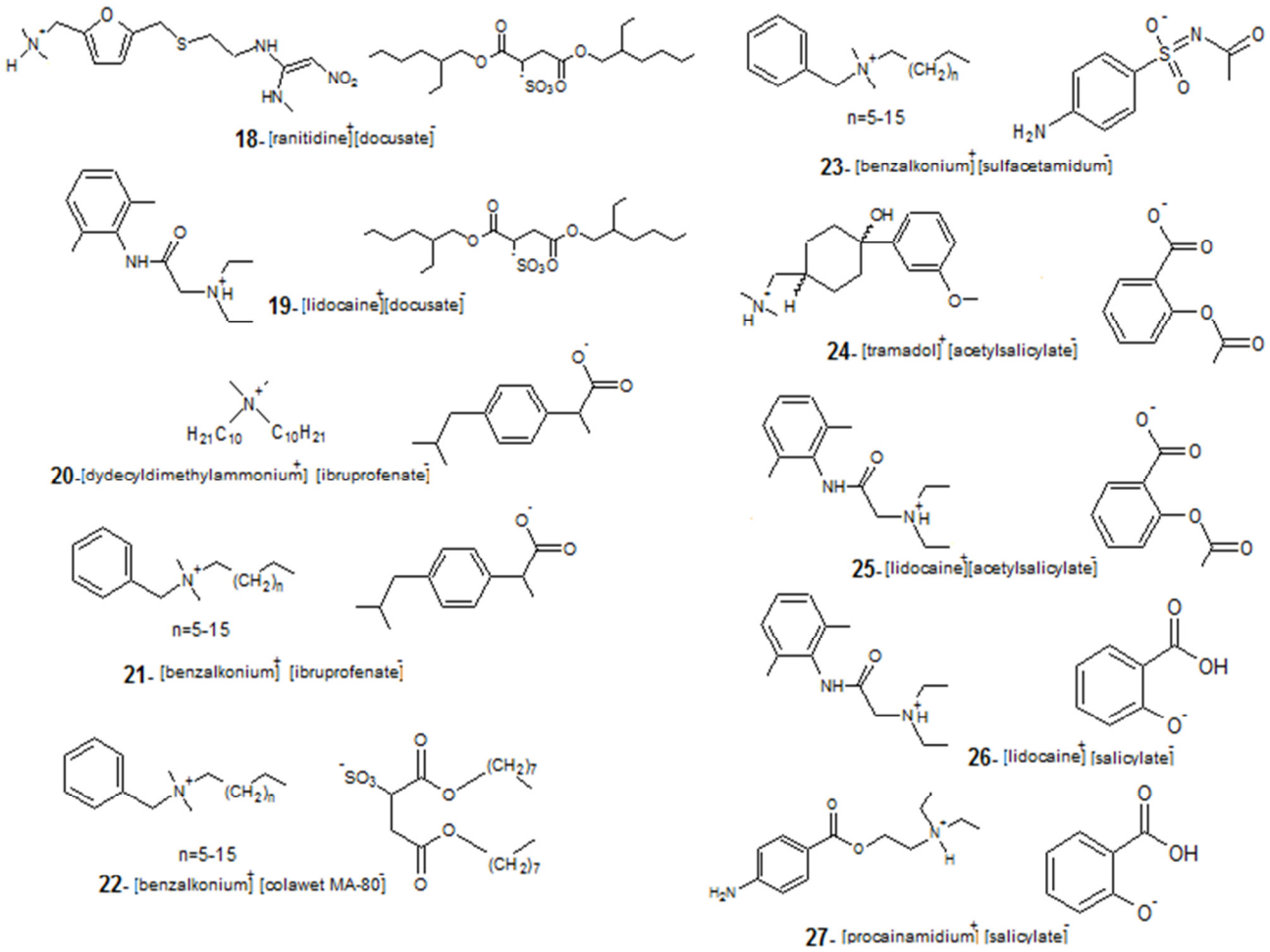

Figure 1.5 - Examples of ILs derivated of APIs [54, 90, 91].

Figure 1.5 illustrates some examples of ILs based on APIs that combine diverse properties. The IL **22**, is an antibacterial combined with a wetting agent used in agriculture resulting in increased lipophilicity of the benzalkonium cation with antibacterial properties [90]. Sulfacetamidium, the active ion in Sulfacetamide, is a sulfonamide antibiotic used in acne treatment that is exclusively commercialized as a sodium salt. Combining this antibiotic with the benzalkonium cation can result in a IL (**23**) with broader spectrum of action [90]. Procainamide is an antiarrhythmic and has recently been combined with salicylate anion to form the IL **27** with multiple functions: antiarrhythmic, analgesic, anti-inflammatory and antipyretic [91].

ILs, as APIs, have enormous potential of development. The majority of the 2009's top 200 selling drugs can be, with the right counter-ion, turned into ILs [92]. This can lead to countless new formulations, properties and, as the case with Lidocaine ducosate, new therapeutical mechanisms that can bring a whole new range of opportunities.

1.3 Immobilization of ILs

ILs are being developed and used for a wide range of applications. Despite all the advantages, ILs have two major drawbacks: high viscosities and cost. These disadvantages can be attenuated with the immobilization of ILs in solid supports [93, 94]. Economically and environmentally, immobilization of ILs can be of extreme interest, resulting in more efficient use of ILs, possibility of recycling, saving costs and resources [94]. One of the main uses of supported ILs is in catalysis where supported ILs catalysis combines the advantages of ILs with the advantages of heterogeneous catalysis [95]. ILs have been immobilized in inorganic (silica, zeolites) and organic (polymers, carbon nanotubes) for various applications such as solar and fuel cells or analytical chemistry [36, 45, 95-101].

Immobilization of ILs based on APIs has also been studied for the development of drug delivery systems.

Failure in drug formulation, an industrial challenge and a difficult task, is responsible for the majority of negative outcomes of clinical trials, owing to drug's inability of reaching the targeted site of action [102]. Most of the administrated drugs are administrated over tissues or organs that are not involved in the pathological process (oral route, for example), often leading to several and severe side effects [102]. Drug delivery systems can minimize drug loss, increase therapeutic efficacy through improved pharmacokinetics and a more efficient distribution of the carried drug [102]. Natural or synthetic polymers, lipids for liposomes, surfactants, dendrimers or ionogels are usual drug carriers for drugs [103-107].

Even though IL immobilization can also be used to develop drug delivery systems, there is a limited number of studies regarding that application. Trewyn *et* al. used methylimidazolium-based as template for the synthesis of mesoporous silica nanoparticles [108]. The mass transport and controlled release patterns of ILs were analyzed by the antibacterial activity of the nanoparticles against *Escherichia coli K12.* Nanoparticle's pore size and morphology were crucial factors for the controlled release of the antibacterial ILs [108]. Ionogels containing [bmim][ibuprofenate] were synthesized by a simple one-step sol-gel procedure and were found to be a good alternatives for controlled drug delivery systems [107]. Release kinetics were slower with ionogels than with crystalline ibuprofen or pure IL, showing their potential as drug reservoir and a drug delivery systems with controlled release patterns. Polymerized ILs can also be used for drug delivery and gene vector for gene therapy. Zhang *et* al. synthetized poly[3-butyl-1-vinylimidazolium][L-proline] and discovered that the imidazolium cation has high binding ability to DNA and it protected it against enzymatic degradation, being also effective transferring the reporter gene to cells [109].

IJ has also the potential to be used as a support for the delivery of ILs based on APIs. For drug delivery applications, natural polymers are seen as an excellent option, despite variation of properties from different sources or danger of infections [110]. Their excellent biocompatibility, ability to mimic native cellular environments, mechanical properties and biodegradability are much appreciated characteristics for biomedical applications [111].

1.4 Electrospinning

Electrospinning is the process that uses electrostatic charges with the objective of producing fibers from polymer melts or polymer solutions [112]. Usually, an electrospinning setup consists of a high voltage supply, a syringe pump, a syringe equipped with a capillary needle coaxially positioned at the center of a conductive ring and grounded collector.

The electrospinning process uses a high voltage supply to charge the polymer melt or polymer solution. When submitted to high voltage, the liquid droplet formed at the tip of the capillary becomes charged and repulsive interactions between equal charges take place. At the same time attractive forces exerted by the oppositely charged collector start to deform the liquid drop at the tip of the capillary. When the electrostatic forces surpass the drop's surface tension one can observe the formation of the Taylor cone [112]. If the solution parameters are appropriate, a fiber jet is formed and pushed out from the Taylor cone, being submitted to bending instabilities until it reaches the grounded collector. These bending instabilities increase the path length and transit time to the collector, allowing solvent evaporation and fiber thinning process [112].

Some biotechnology applications, such as drug delivery systems or tissue engineering, usually rely on nanoscale or sub-micrometer structures because of their unique properties like increased surface area [113]. Some of these systems are composed of polymer fibers and electrospinning is the easiest, simplest and most straightforward technique to produce fibers that can reach nanometer sizes [114]. Fibers of those diameters can mimic the structural dimension of the extracellular matrix of various native tissues and organs or have a high drug concentration for drug delivery [115].

Electrospun fibers have been used for countless applications of drug delivery systems, like controlled release of retinoic acid using PGLA as a biodegradable polymer [104] or gene silencing via controlled release of siRNA using PCL [103].

The possibility of using a wide range of polymers and solvents to produce fibers is an attractive factor of the technique [112, 113]. Viswanathan *et* al. took advantage of cellulose's solubility in [bmim][Cl] to produce cellulose and cellulose-heparin composite fibers, combining the advantages of biopolymers with the unique properties of ILs [116]. Gelatin has been already

electrospun but there are few reports in the literature. Huang *et* al. produces gelatin fibers in a solution of 2,2,2-trifluoroethanol [115]. Ki *et* al. also reported gelatin fibers produced from a formic acid solution, but polymer degradation was observed [117]. Zhang *et* al. obtained gelatin fibers in aqueous solutions, verifying that temperature is an important factor in gelatin electrospinning process [118].

IJ has already been electrospun by co-workers of our group [119]. An electrospinning process was optimized for the fiber production of IJ fiber using [C_2OHmim][BF_4]. The new properties like increased surface area and high conductivities of electrospun microfibers open up a vast range of possible applications for IJ.

1.5 Objectives

Owing to their tunable properties, ILs have a broad range of possible applications. ILs have begun their way towards different applications other than electrolytes or solvents for green synthesis. ILs are now seen as an interesting alternative to crystalline APIs which have their efficacy limited due to polymorphism. Avoidance of polymorphism and the recent interest of developing new drug delivery strategies, have led to studies regarding ILs' immobilization as a safe and effective way of maximizing drug efficacy and formulation. As stated above, ILs have some drawbacks like high viscosities and environmental concerns, which can limit their practical applications. Recently, new ions have been proposed in order to create cleaner and more environmental friendly ILs. Choline salts have been gathering relevant attention precisely for their reduced environmental danger. Moreover, there are some studies regarding choline cation derivates and the assessment of their biological properties [64, 65]. It is known that functionalization of choline cation modifies the biological properties of some ILs, suggesting different cell membrane interactions, improved lipophilicity and consequent effectiveness increase [64, 65].

In this work we explore the immobilization of choline-based ILs in membranes composed of IJ electrospun fibers in order to improve the effectiveness of ILs. Electrospinning is a simple and straightforward technique for the production of porous membranes with high surface area and its applicability to produce IJ fibers has already been studied in our group with positive outcomes [119]. Mandelic acid, IL – [Ch][Ma] and electrospun fibers containing this IL (IJ-[Ch][Ma]) are tested as antibacterial agents and their effectiveness and efficiency is compared in order to evaluate the potential of electrospinning as a way of producing IJ membranes for drug delivery applications.

2 MATERIALS AND METHODS

2.1 Chemicals used

2.1.1 IL

The choline-based ILs used for this work were previously synthesized in the laboratory.

The IL choline acetate (IL – [Ch][Ac]) has its structure displayed in **Figure 2.1**.

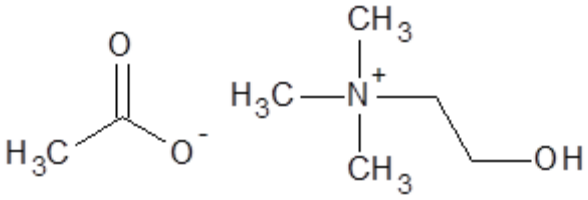

Figure 2.1 – Chemical structure of IL – [Ch][Ac].

The IL choline mandelate (IL – [Ch][Ma]) has its structure displayed in **Figure 2.2**.

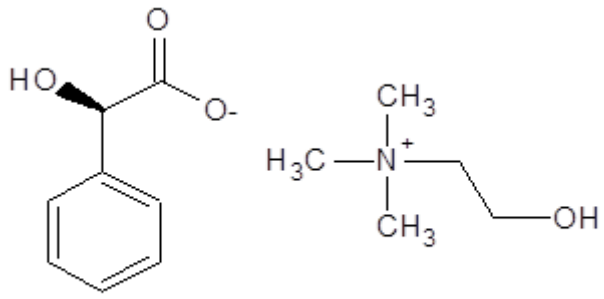

Figure 2.2 – Chemical structure of IL – [Ch][Ma].

The IL choline tiglate (IL – [Ch][Ti]) has its structure displayed in **Figure 2.3**.

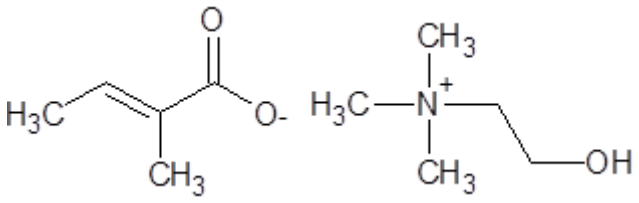

Figure 2.3 – Chemical structure of IL – [Ch][Ti].

The IL choline ibuprofenate (IL – [Ch][Ib]) has its structure displayed in **Figure 2.4.**

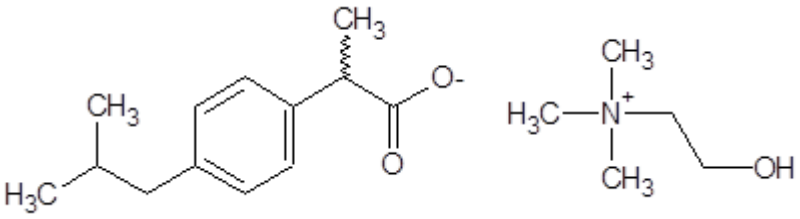

Figure 2.4 – Chemical structure of IL – [Ch][Ib].

Other ILs were used for solubilization of DNA and N,N- dimethylchitosan. The IL [bmim][Cl] (99%) was purchased from Io-li-tec, while [C_2OHmim][BF_4] (≥ 98%) was purchased from Solchemar.

2.1.2 Other chemicals

The gelatin used for IJ formation was bacteriological gelatin 403902 by Cultimed. Choline Chloride used in the antimicrobial activity tests was provided by Fluka (≥ 97%). R – (-) - Mandelic acid (98%) used in the same antimicrobial tests was purchased from Fluka.

Purified Calf Thymus DNA-Na salt was purchased from Merck (Calbiochem). Salmon milt DNA was purchased from TCI. N,N-dimethylchitosan was synthetized in the laboratory (Chitosan deacetylation degree 90%, M_w= 200 – 350)

Distilled water was distilled in the laboratory. Absolut ethanol was purchased from Riedel-de Häen.

2.1.3 IJ solutions

The IJ solutions used for IJ formation/DSC and the optimized solutions for electrospinning/tensile tests are described below:

Table 2.1 – Quantities of water and gelatin used for the formation of IJ solutions.

IL	IJ formation / DSC		Electrospinning / Tensile tests	
	Water (µL)	Gelatin (mg)	Water (µL)	Gelatin (mg)
[Ch][Ac]	134	40	682	204
[Ch][Ma]	124	40	432	130
[Ch][Ti]	130	40	660	198
[Ch][Ib]	116	40	435	131

Note: The IL volume added was always 100 µL.

The procedure for the preparations of the IJ solutions began with the addition of the desired IL volume to a vial with a magnetic stirrer. Gelatin was then added and mixed afterwards with the IL for 5 minutes to stabilize temperature and enable some gelatin solubilization. Last step was the addition of distilled water at 55ºC, followed by stirring for a minimum time of 30 minutes or until the solution was found to be homogenized. The "R" ratio that characterizes a given IJ is the ratio between the volume of IL (µL) and gelatin weight (mg).

For the preparation of IJ dense films for DSC and tensile tests, the IJ solutions were cautiously spread with a spatula in a warm microscope slide and left to rest for a minimum time of 48 hours at room conditions. For the electrospinning process, the warm IJ solutions were rapidly put in a warm syringe in order to prevent gelification.

2.1.4 Electrospinning

The experimental setup used for this work is shown in **Figure 2.5**.

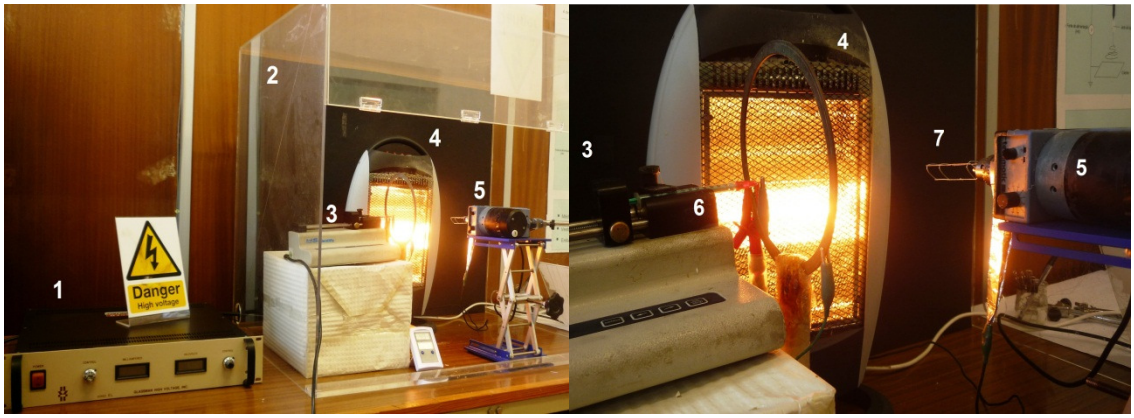

Figure 2.5 – Electrospinning setup used for the electrospinning of IJ solutions.

For this electrospinning setup, the high voltage supply used was a Glassman EL 30 kV (**Figure 2.5 – 1**). This high voltage supply positively polarized a capillary needle with an internal diameter of 0,26 mm put in a syringe (**6**). The syringe pump used was a KDS100 by KD Scientific (**3**). A drill (**5**) was used as a rotating motor for the wire grids that were used for the

rotating grounded collectors (**7**). All this equipment was located inside an acrylic box in order to control temperature and humidity (**2**). An electric heater (**4**) was used to keep temperatures high enough (around 40ºC) to prevent gelatin solidification. Despite evidence that higher temperatures have a decreasing effect on gelatin fibers, Zhang *et* al. verified fiber degradation when the temperature was too high [118]. To prevent degradation and gelatin solidification, the electrospinning temperature was kept at the lowest possible. For all experimentations, humidity was always kept around 20%.

2.1.5 DSC

Differential scanning calorimetry (DSC) is the most used technique to perform thermal analysis. In heat-flow DSC, during temperature variation, the difference in heat flow between a sample and a reference is measured and registered [120]. When a phase transtition takes place in the sample at a given temperature, more or less energy is required to keep the sample temperature the same as the reference one. This enables DSC to measure events like physical transformations (melting points, crystallization temperatures) and related enthalpies, for example.

DSC results were obtained with a differential scanning calorimeter Seteran DSC131 with a temperature variation rate of 20ºC/min. Two cycles were performed and samples were kept at 90ºC for 5 minutes between them. Results shown only account for the second heating cycle.

2.1.6 UV/Vis spectroscopy

UV/Vis molecular absorption spectroscopy is a widely used technique for analytical quantification of various types of compounds. It is an especially useful technique to quantificate conjugated organic compounds.

Quantification of IL – [Ch][Ma] was performed in a Beckman Coulter DU – 800 spectrophotometer.

The calibration curve for the IL quantification was obtained with the absorbance readings of four IL – [Ch][Ma] standards. The blank used was a gelatin aqueous solution. **Table 2.1** summarizes the concentrations of the standards and the blank solution.

Table 2.2 – Solutions used for UV/Vis spectroscopy calibration curve.

IL – [Ch][Ma] standards	Gelatin blank solution
[0,15; 0,30; 0,60; 1,20] mg / mL	Aqueous solution 0,4 mg / mL

2.1.7 Tensile tests

The uniaxial tensile test is a routinely used test performed in materials science to evaluate mechanical properties of a material. The test provides critical information like stress at break, strain at break and Young's modulus [121]. During the test, the elongation is recorded against the applied force.

The experimental setup is depicted in **Figure 2.6**

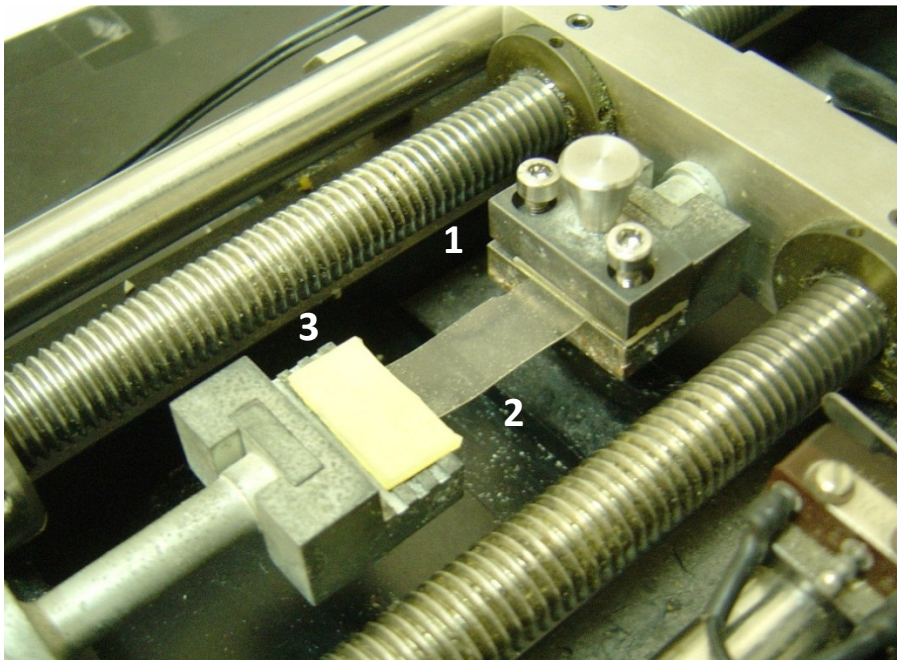

Figure 2.6 – Tensile test setup used for IJ tensile testing.

The setup described in **Figure 2.6** shows how a wedge grip (**1**) holds the IJ membrane (**2**) in place and aligned to applied force direction. A rubber strip (**3**) was used to prevent IJ membrane to slip.

The mechanical properties of IJ films were registered with the tensile testing machine Rheometric Scientific Minimat, Firmware 3.1 at room temperature. The IJ dense films, cut into rectangles with 3x1 cm, were stretched at constant speed of 5 mm/min until rupture. IJ films thickness were measured with a Mitutoyo digital micrometer and the thickness values presented are a mean value of 5 measures.

2.1.8 Fiber Characterization

2.1.8.1 Optical Microscopy

Optical microscopy (OM) is the simplest type of microscopy and uses visible light and a lens system to magnify images. The light, passing through a condenser, samples, objective lenses and the ocular lens, allows a magnified visualization of samples or details with small dimensions.

OM was used in this work to analyze IJ fibers during the electrospinning parameters optimization. The optical microscope used was an Olympus BH-2. The magnification powers used were 40x and 100x for the unoptimized and optimized IJ fibers, respectively.

2.1.8.2 Scanning Electron Microscopy

Scanning electron microscopy (SEM) is a type of microscopy that uses a beam of high-energy electrons. The beam is produced, usually, by a tungsten filament and has energy values ranging from 0,5 to 40 keV. Once the electron beam hits and interacts with the sample, other signals are produced like secondary electrons, X-rays or backscattered electrons. This variety of signals provides valuable and vast information about the sample being secondary electrons those which produce SEM images. The samples must be solid and electrically conductive. Nonconductive materials are coated with an ultrathin layer of a conducting material.

SEM was the technique used to analyze the electrospun fiber samples through high resolution images. The fibers were coated with a gold/palladium alloy with a Polaron SC502 sputter coater and the microscope used was a Zeiss DSM 962. Samples were suspended over two strips of carbon conductive tape purchased from Agar Scientific.

2.1.9 Antimicrobial Activity

The agar diffusion test, or Kirby-Bauer disk diffusion method, was used to demonstrate the antimicrobial potential of IL – [Ch][Ma]. The test is performed in an agar culture plate, where growing bacteria are put in contact with a sterile paper disk containing the antibacterial agent. Inhibition is observed when a bacteria clear zone is observed around the paper disks. That zone of inhibition is the zone where bacteria were incapable of growing in the presence of the antibacterial agent.

The bacteria used for the agar diffusion tests were *Bacillus subtilis* 168 (*B. subtilis*) and *Escherichia coli* K-12 (*E. coli*). Both were pre-inoculated in 5 mL of LB medium[122] and incubated for 16 hours in a Sanyo orbital incubator Orbi-Safe Ts. For all antimicrobial tests, the pre-inoculums were first diluted in LB medium in a 1:50 proportion prior the inoculation of agar plates (containing LB medium (LAB M) with 1,6% w/v of agar concentration) except mentioned otherwise. Paper disks (diameter = 6 mm) and IJ fibers were put in agar plates inoculated with 100 µL of the previously diluted pre-inoculum and were incubated during the first 3 hours at room temperature followed by an overnight incubation at 37ºC.

2.1.10 Karl Fischer Titration

Karl Fischer (KF) titration is a widely used method for water quantification in a vast range of applications. This is a coulometric titration which checks the oxidation of sulfur dioxide by iodine in the presence of water, an alcohol and an organic base. During titration, iodine concentration is checked. When the reaction end-point is reached, a sharp increase of iodine concentration is detected. The total amount of current needed for iodine formation is recorded throughout the assay, allowing water quantification.

Karl Fischer titrations were carried out at room temperature with a Metrohm 831 KF Coulometer. Values presented are the mean values of three measures.

2.1.11 Dielectric relaxation spectroscopy

Dielectric relaxation spectroscopy (DRS) is a technique that analyzes relaxation events like dipole movements caused by the application of an electric field. DRS was used to measure conductivity values of ILs.

Two silica spacers with 0,05 mm were put between two gold plated electrodes. The IJs and the gold electrodes were put in a Novocontrol BDS 1200 parallel placed capacitor. Assay temperature control was performed with a BDS1100 cryostat part of Quatro Cryosystem by Novocontrol. Heated gas stream was evaporated from liquid nitrogen in a Dewar. Measurements were performed in an Alpha-N analyzer from Novocontrol GmbH (frequency range from 10^{-1} Hertz to 1 Mega Hertz).

3 RESULTS AND DISCUSSION

3.1 Ion Jelly formation.

The first aim of this work was to evaluate if the choline-based ILs were able to form IJs. This is a critical feature to produce IJ fibers through electrospinning. It was found that all choline-based ILs formed solidified gels with the following concentrations:

Table 3.1 – Concentrations of IL and gelatin for IJ formation.

IL	% IL v/v_{water}	% gelatin w/v	R (v IL /m gelatin)
[Ch][Ac]	75	30	2,5
[Ch][Ma]	81	32	2,5
[Ch][Ti]	77	31	2,5
[Ch][Ib]	86	34	2,5

Despite the fact that all ILs formed solidified gels, IJ – [Ch][Ti] and IJ – [Ch][Ma] took a longer time to jellify completely. On the other hand IJ – [Ch][Ac] and IJ – [Ch][Ib] formed more brittle and noticeably stronger films and their jellification took place right after the spread of IJ solution in a warm microscope slide glass. **Figure 3.1** shows the example of IJ – [Ch][Ti] spread over a microscope slide glass and the respective difficulty in the jellification process.

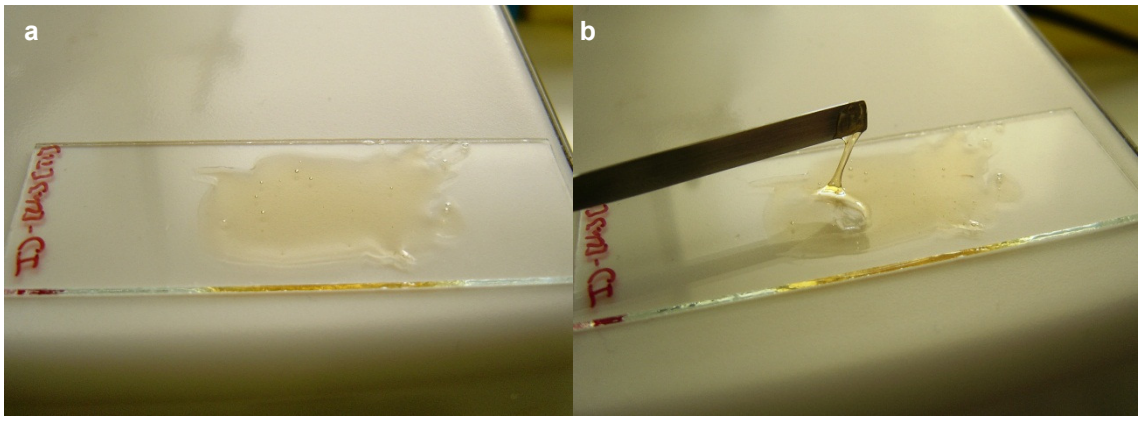

Figure 3.1 – IJ – [Ch][Ti] spread over a microscope slide glass (a). The right image (b) is the same IJ 5 minutes after spreading still sticking to the spatula.

3.2 DSC analysis

Both choline-based ILs and the resulting IJs were submitted to DSC analysis to analyze their phase transitions. The thermograms are depicted in **Figure 3.2**.

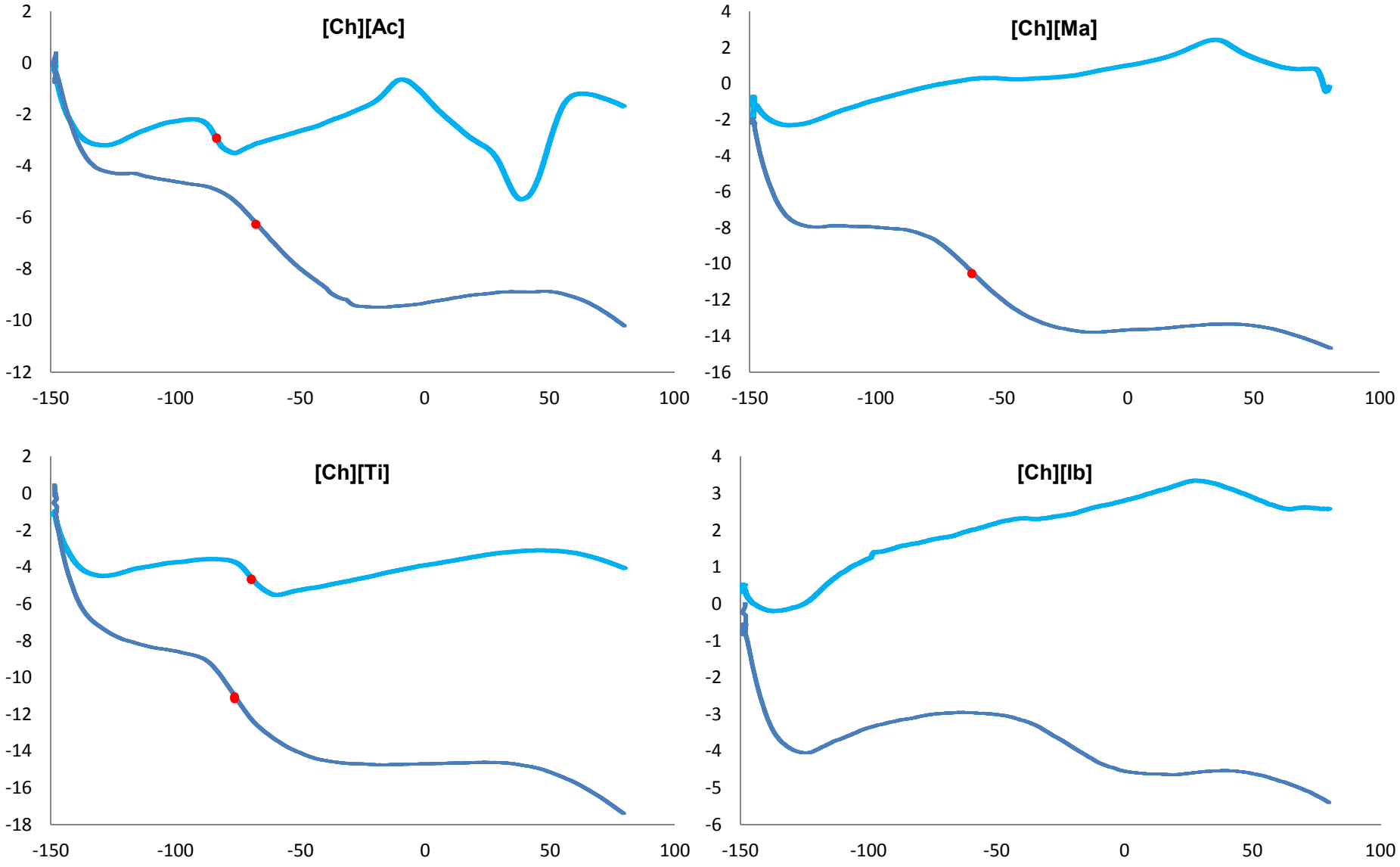

Figure 3.2 – DSC curves of ILs and IJs (IJ , IL, T_g, ↑exothermic, abscissa units: W/g, ordinate units: ºC).

Table 3.2 – Glass transition temperatures (T_g) detected from DSC analysis.

	T_g (ºC)	
	IL	IJ
[Ch][Ac]	-84,5	-68,6
[Ch][Ma]	-	-62,3
[Ch][Ti]	-70,7	-78,6
[Ch][Ib]	-	-

The thermograms reveal that the IJs keep their structural properties in a wide range of temperatures, including usual room temperatures and also normal human body temperature. This is an important factor to consider given the potential use of these IJs for drug delivery applications. For the range of temperatures displayed it is not observed melting point for any IJ or IL. The endothermic peak for IL – [Ch][Ac] at 37ºC suggests a transition state that apparently resembles a melting point. In reality IL - [Ch][Ac] is liquid below 37ºC and around room temperatures. Knowing the IL's hygroscopicity, this endothermic peak can be related with water evaporation from IL. Noteworthy is also the absence of endothermic peaks in the IJs curves related to denaturation of gelatin's triple-helix crystalline structure. Bigi *et* al. verified that various gelatin samples (with and without cross-linking) showed a denaturation temperature around 41 ºC [123]. The absence of endothermic peaks in this region suggests that ILs interact in a different way with gelatin, preventing the polymer chains to renaturate upon cooling.

Vitrification temperatures (T_g), displayed in **Table 3.2,** are observed for IL – [Ch][Ac] (T_g= - 84,5ºC), IL – [Ch][Ti] (T_g= - 70,7ºC), but not for IL – [Ch][Ib] and IL – [Ch][Ma]. All IJs exhibit a T_g with the exception of IJ – [Ch][Ib] (despite having a slight curve inflection on the thermogram curve around – 25ºC). From the **Figure 3.2** it is noticeable that IJ – [Ch][Ac] has a T_g= - 68,6 ºC and IJ – [Ch][Ti] has its glass transition at T_g= - 78,6 ºC. Even though IL – [Ch][Ma] did not exhibit glass transition temperature, the resulting IJ – [Ch][Ma] has a T_g= - 62,3ºC.

Our results show that most of IJs exhibit a T_g when compared with ILs and the T_g value is always obtained at a higher temperature when compared with the pure ILs. This fact was also verified by Carvalho *et* al. when compared pure [bmim][dca] with two different IJs produced with this IL [124]. For instance $[bmim][dca]_{r=1,1}$, exhibits a T_g of -63ºC. Nevertheless when we increase three times the amount of IL $[bmim][dca]_{r=1,1}$ the Tg decreases to nearly -100 ºC which is the T_g value of the pure IL. These results might suggest that the presence of gelatin increases the capability of IL to become a glass former. This is probably due to the strong ionic interaction between gelatin and IL.

3.3 Electrospinning

Gelatin is not an usual polymer used for electrospinning process because of its high degree of hydrogen bonds. High polar solvents, acidification or temperature increase are good and successful strategies for attenuating intermolecular interactions [115, 117, 118].

The IJs precursor solutions described in **Table 3.1** were tested in the electrospinning apparatus described in section **2.1.4**. To prevent the solidification of the IJs solutions and their spinnability, the working temperature was always kept slightly above 40ºC in the electrospinning chamber with the use of the electric heater already mentioned in section **2.1.4**.

It was not possible to obtain good results from the aforementioned IJ solutions. From the solutions displayed in **Table 3.1,** only IJ – [Ch][Ma] and IJ - [Ch][Ib] produced fibers, regardless of their instability and the extremely low yield. These preliminary results are summarized in **Table 3.3**.

Table 3.3 - Preliminary electrospinning conditions for IJ solutions.

IJ - Solution	Voltage (kV)	Distance to collector (cm)	Flow (mL/h)
IJ – [Ch][Ma]	10,1	6	0,65
IJ – [Ch][Ib]	9	10	0,40

The fibers produced with the conditions summarized on the above were unstable and collapsed after a short period of time. This inability to produce fibers suggested that the relative concentrations of gelatin and IL should be tuned in order to obtain fibers. The next step was to perform a fine tuning of the IJ concentration in the IJ composition.

3.3.1 Gelatin concentration

Gelatin concentration was the first parameter to be tuned.

For all the choline-based ILs, a range of gelatin concentrations was tested for electrospinning. It was soon discovered that a decrease in gelatin concentrations would render ineffective. Even small decreases in gelatin concentrations lead to a strong decrease in viscosity. When gelatin concentration is below 25% w/v, fibers can't be produced because the lower polymer concentration hampers chain entanglements to occur [112]. This lack of entanglement will result in electrospraying and droplet production. Low gelatin concentrations will force the polymer fiber to break up into droplets due to higher surface tension and lower viscosity. On the other hand, the increase of gelatin concentration to 40% w/v or more resulted in an increased viscosity which also interferes with the electrospinning process. With these

results in mind, it was chosen not to change in a significant way gelatin concentration and keep it around 30% w/v.

These results for gelatin concentrations are coincident with the outcomes of other electrospinning works of aqueous gelatin solutions [118]. Zhang *et* al. verified electrospinning of solutions with a gelatin content between [30-50]% w/v yielded good results. Electrospinning of gelatin solutions with a concentration of 35 % w/v at 45 ºC were selected as the preferable conditions for the production of gelatin nanofibers [118].

Taking into account the issues discussed above, it was chosen to keep the gelatin concentration values of **Table 3.1** unchanged. The main reason for this choice is related to the influence of polymer concentration on fibers' diameters. As a matter of fact, Zhang *et* al. verified that gelatin fibers' average diameter increased from 125 nm to 211 nm with the increase of gelatin concentration from 30% to 40% (w/v) [118]. With biomedical and drug delivery applications as a main objective for IJ fibers, it is desirable that the fibers have the lowest possible diameter in order not only to increase surface area, but also to maximize the potential of drug controlled release.

3.3.2 IL concentration

After the evaluation and discussion of gelatin concentrations, we turned our attention to IL concentration. Given that gelatin concentrations in IJ solutions were apparently appropriate, we have evaluated the impact that IL had on the electrospinning process.

Taking into account the high concentrations of IL, the first step was to reduce its content in the IJ solutions. IL concentration was lowered to 40% v/v in all cases while maintaining gelatin concentration at 30% w/v. Electrospinning of those new IJ solutions was still very difficult. Nevertheless, the decrease of IL concentration yielded more fibers and they seemed to be slightly more stable, without collapsing. The resulting fibers were analyzed in an optical microscope and the images are depicted in **Figure 3.3 a)-d)**. All the fibers produced have sizes of dozens of micrometers and fiber fusion is noticeable for all cases. This phenomena is particularly evident for the IJ – [Ch][Ib] (**Figure 3.3, image d)**).

The results discussed above lead to further reduction of IL concentration in the IJ solutions. New solutions were prepared with the same gelatin concentration but with a sharp reduction of IL concentrations (23 % v/v). Electrospinning turned out to be much easier, resulting in a sharp increase of fiber production yield. All samples were analyzed with the optical microscope. **Figure 3.3 e)-h)**, clearly shows a dramatic increase of fiber production when compared to fibers depicted in **a)-d)**. It is also noticeable that fiber diameters are lower. This fact is particularly evident for the IJ – [Ch][Ma] and IJ – [Ch][Ib] cases, where the obtained fibers fall in the micrometer range.

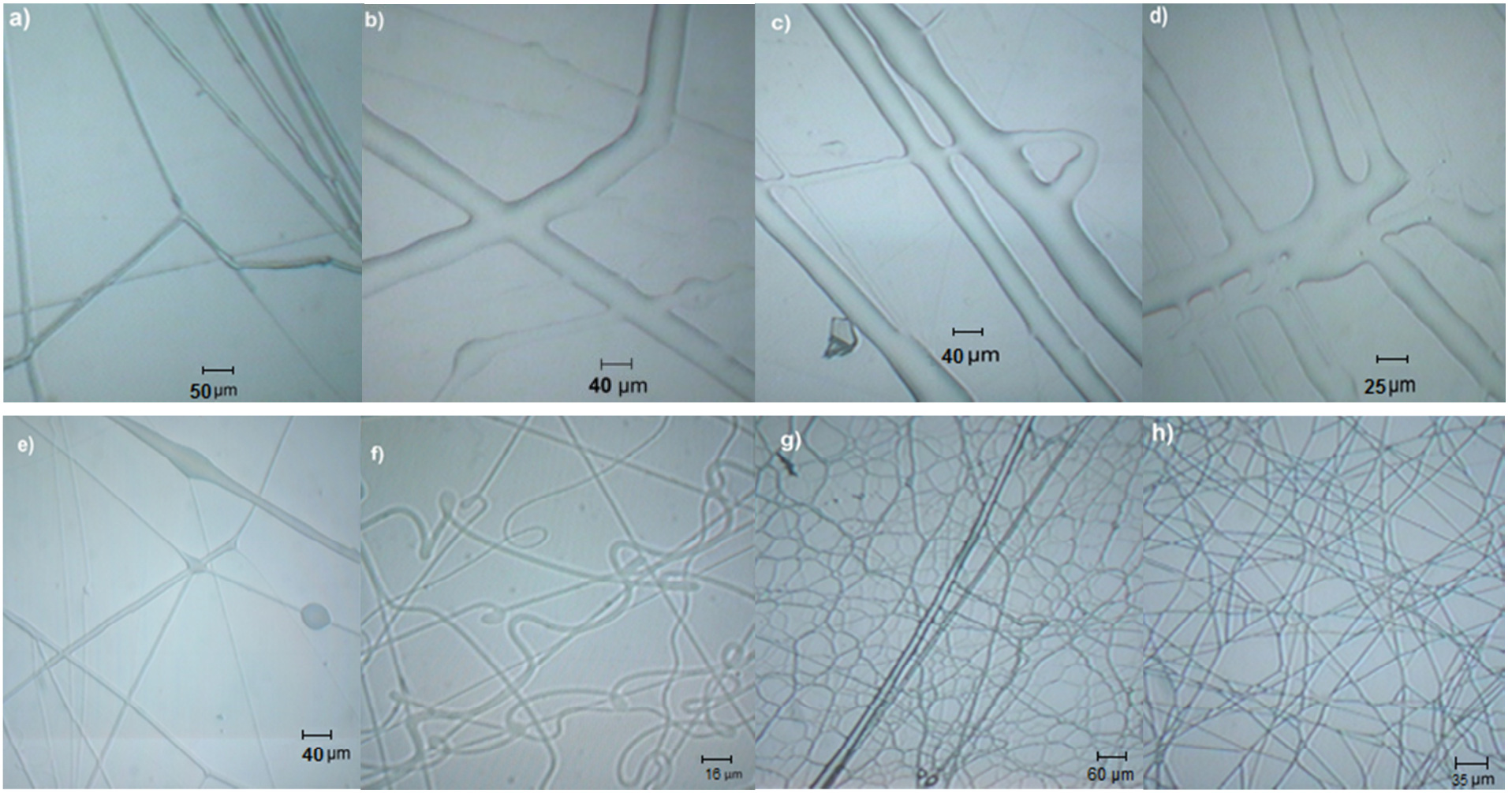

Figure 3.3 – OM images of IJ electrospun fibers. [First row: **a-d)** IL concentration = 40% v/v. Second row: **e-h)** IL concentration = 23% v/v. Images **a,e)** IJ – [Ch][Ac], **b,f)** IJ – [Ch][Ma], **c,g)** IJ – [Ch][Ti], **d,h)** IJ – [Ch][Ib]. Electrospinning: 15 kV, 15 cm, 0,01 mL/h for all IJs but IJ – [Ch][Ti] which needed a flow rate of 0,025 mL/h]

Even with a great reduction on IL concentration for IJ – [Ch][Ac] and IJ – [Ch][Ti], (**depicted in Figure 3.3 e)** and **g)**), we still can observe fiber fusion phenomena. This leads to higher degree of defects and to an increase on fiber diameter when compared with IJ – [Ch][Ma] and IJ – [Ch][Ib] fibers. For the IJ – [Ch][Ti] this phenomena is visible even on the thinner fibers and gives them a unique aspect. For the IJ – [Ch][Ac] it is noticeable that fibers have also beads.

In order to obtain better electrospun fibers for IJ – [Ch][Ac] and IJ – [Ch][Ti], IL concentration was reduced again. New IJ solutions were prepared with a gelatin concentration of 30% w/v and IL concentration of 15% v/v. The new IJ solutions were electrospun with the same conditions as the ones presented in **Figure 3.3** (15 kV, 15 cm). The reduction on IL concentration led to the elimination of the above mentioned fiber fusion phenomena. The result is a much higher fiber number and a sharp decrease on fiber diameters, as demonstrated in **Figure 3.4**.

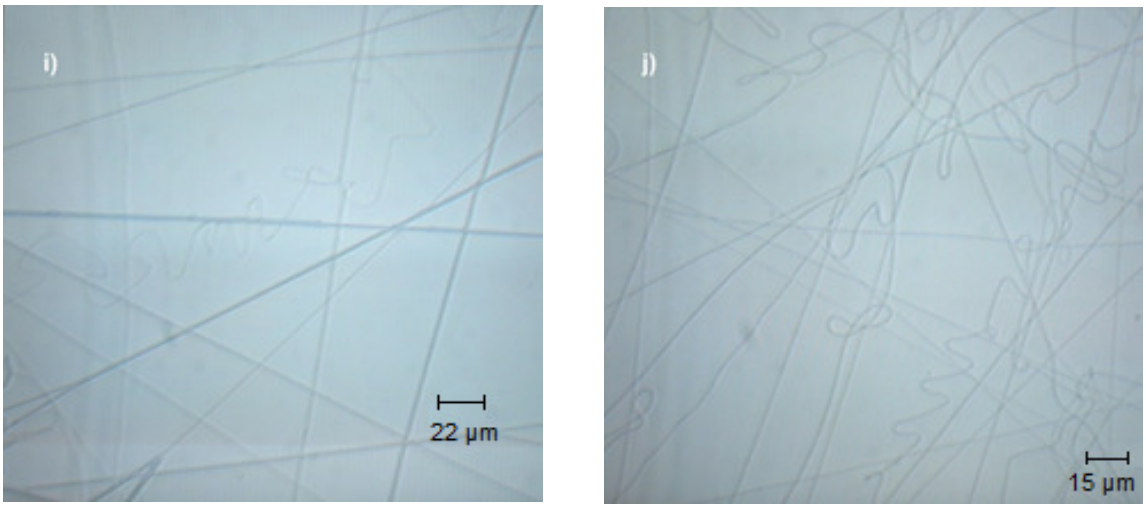

Figure 3.4 – OM images of IJ electrospun fibers. [IL concentration = 15% v/v. **i)** IJ – [Ch][Ac], **j)** IJ – [Ch][Ti]. Electrospinning: 15 kV, 15 cm, 0,01 mL/h except IJ – [Ch][Ti] which needed a flow rate of 0,018 mL/h]

A possible explanation for the decrease of fiber fusion and diameter with the reduction of IL concentrations is related with the polymer solution conductivity. Arumugan *et al*. have already studied the fiber fusion phenomena in PVA and PLA solutions with different types of salts [125, 126] . The salt addition resulted in higher conductivities and different fiber behavior during the thinning process. **Figure 3.5** presents the proposed mechanism of fiber fusion by the authors.

A polymer solution without conductive additives is straightly attracted to the collector. In this case (**Figure 3.5 a)**), fibers do not aggregate due to the repulsive forces of the positively charged fiber segments at the surface. The conductivity increase caused by the addition of a salt changes the path followed by fibers on their way to the collector. The increase of polymer

solution's conductivity with further salt addition and the positively polarization during the electrospinning process contributes to the emergence of negative charges at the fibers' surface.

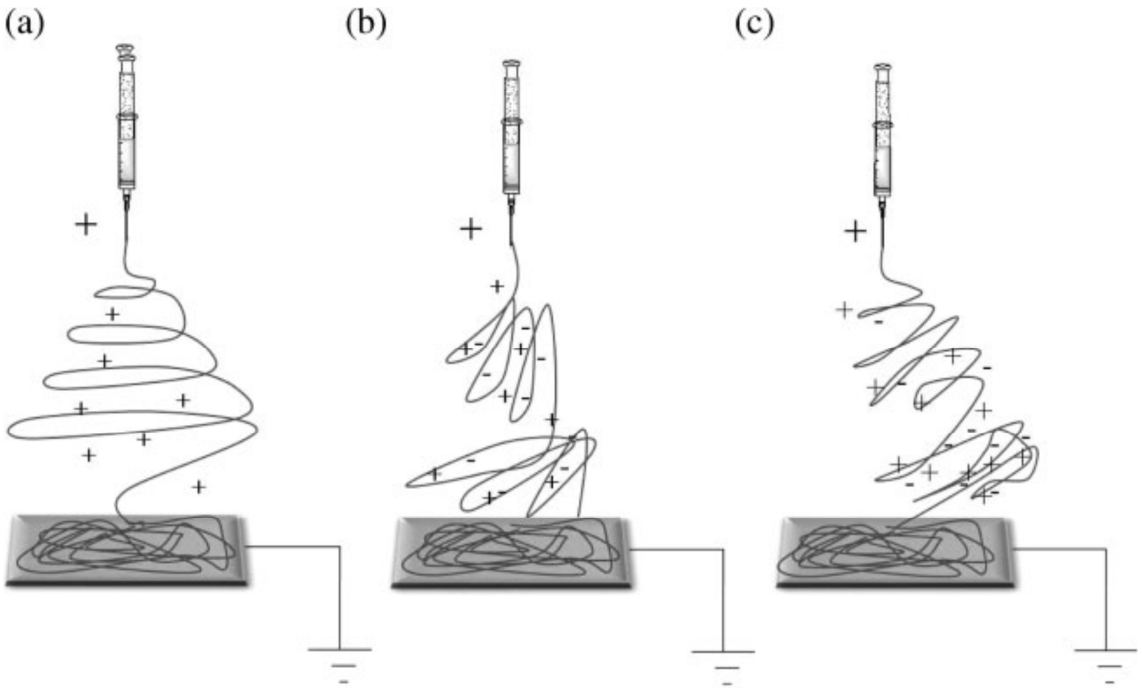

Figure 3.5 – Mechanism of fiber fusion and the effect of high conductivity [125, 126].

The presence of negative charges in some fiber segments attract their positively charged counterparts nearer the tip of the capillary needle, contributing to fiber fusion and diameter increase (**Figure 3.5 b)** and **c)**). The fibers are attracted to the grounded collector only after the fusion phenomena. For IJ electrospinning the fusion phenomena is visible, especially when working with high IL concentrations.

During the thinning process it was possible to observe the formation of a continuous "fiber-cloud" between the tip of the capillary needle and the grounded collector. This cloud effect was greatly reduced with the decrease of IL concentration. This suggests that the "fiber-cloud" could effectively be the visual confirmation of fiber fusion for the electrospinning of highly conductive IJ solutions. The results obtained for the IJ solution and relative concentrations of IL are consistent with this mechanism proposed by Arumugam *et al* [125, 126]. The increase of IL concentration leads to an inevitable increase of conductivity which clearly hampers thin fiber production.

Conductivity measures of IJ solutions were performed to corroborate Arumugan *et* al's theory about fiber fusion [125, 126]. Conductivity values are summarized in **Table 3.4**:

Table 3.4 – Conductivity values of IJ solutions at 25ºC.

IL	σ' (S/cm)
IJ – [Ch][Ac]	$3{,}48 \times 10^{-4}$
IJ – [Ch][Ma]	$3{,}09 \times 10^{-4}$
IJ – [Ch][Ti]	$6{,}45 \times 10^{-4}$
IJ – [Ch][Ib]	$3{,}69 \times 10^{-5}$

Conductivity values obtained by DRS corroborate fiber fusion theory proposed by Arumugam *et* al [125, 126]. IJ – [Ch][Ti] and IJ – [Ch][Ac] exhibit higher conductivity values compared to the other IJs. Their higher conductivity is related to reduced anions' size and interaction between the IL and gelatin. In spite of acetate's being shorter than tiglate, IJ – [Ch][Ac]'s conductivity is about half of IJ – [Ch][Ti]. This difference is possibly related with the distinct mobility and diffusion of cation and anion on IJ matrix [124]. However, this hypothesis should be confirmed through DRS.

As a matter of fact, IJ -[Ch][Ac] and IJ [Ch][Ti] were the IJs that needed a reduction of IL concentration to 15% IL v/v to reduce fiber fusion phenomena to acceptable levels.

The lower conductivity values obtained for IJ – [Ch][Ma] and IJ – [Ch][Ib] can be explained by their increased ion's size. Mandelate and ibuprofenate anions have a phenyl group in their structure which hampers ion mobility. Not surprisingly, IJ – [Ch][Ib] exhibits the lowest conductivity value which is related to the fact of being the biggest anion.

The reduced conductivity of IJ – [Ch][Ma] and IJ – [Ch][Ib] solutions enabled their electrospinning with IL concentrations of 23% v/v.

These data corroborate the theory that higher conductivities lead to increased fiber fusion as proposed by Arugumam *et* al [125, 126].

Surface charge of ILs aqueous solutions is also dependent of the IL concentration. Sung *et al.* investigated the surface properties of [bmim][BF_4] and water [127]. For a very low range of [bmim][BF_4] concentrations, the surface is covered with $[bmim]^+$ cations. The increase of [bmim][BF_4] concentration results in different surface properties, including surface tension, because anions start to appear at the surface. This presence of negative charges at the surface of the aqueous solution can also have an important impact in the fiber fusion phenomena described above.

The reduction of fiber fusion and fiber diameters with the decrease of IL concentration can be also related to solvent volatility. Solvent volatility is a critical feature for fiber thinning and

fiber deposition in electrospinning. When the fiber jet is accelerated to the grounded collector, the solvent starts to evaporate, leading to fiber solidification and thinning. ILs, as mentioned before, have very low volatility and a solvent with a lower IL content is easier to evaporate than a solvent with an higher IL concentration. The diameters of fibers produced from IJ solutions with an IL concentration of 40% v/v is higher than those produced from IJ solutions with an IL concentration of 23%. The results presented above show that IL concentration is positively correlated with fiber diameter.

Taking into account the results discussed above, it was concluded that the optimal IJ solution compositions are the ones described in the following table:

Table 3.5 – Optimized compositions for electrospinning of choline-based IJ solutions.

IJ - Solution	% IL v/v	% gelatin w/v
IJ – [Ch][Ac]	15	30
IJ – [Ch][Ma]	23	30
IJ – [Ch][Ti]	15	30
IJ – [Ch][Ib]	23	30

.

3.3.3 Electrospinning parameter optimization

Electrospinning is considered to be simple and easy technique to produce fibers. Despite this ease of use, fiber production through electrospinning is affected not only by the polymer solution properties, but also by electrospinning processing parameters.

3.3.3.1 Fiber collector

Three types of collectors were tested for the electrospinning of IJ solutions. The first one tried out was a static metallic wire grid. Fibers were collected using the collector, but the membrane final structure was pretty much disorganized. There was also collage evidence between the two membranes formed around the wire.

To produce more organized IJ fiber membranes the same metallic wire grid was put in a rotating drill. The wire had a triangular prism shape to prevent collage of different fiber membrane faces (**Figure 3.6**). The outcomes were improved with this type of collector and the membrane presented a much more organized pattern, which is preferable owing to improved mechanical properties.

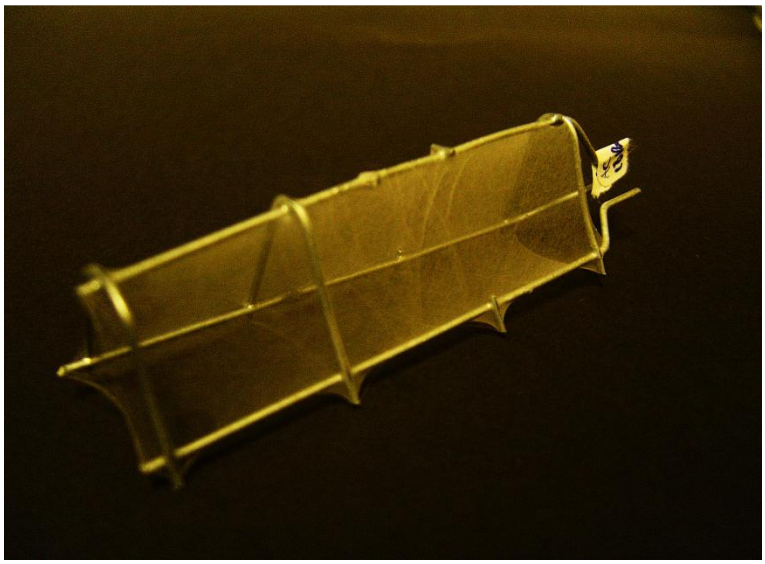

Figure 3.6 – IJ electrospun fibers on a triangular prism shaped collector.

Finally, a plastic grid was tested as fiber collector, but no fiber deposition was observed. The plastic grid insulation is the most probable reason for this result, as the grid would not be charged during the electrospinning process in order to attract fibers.

3.3.3.2 – Applied voltage

The applied voltage is a critical parameter for a successful electrospinning process. The minimum voltage for Taylor cone formation was approximately 9 kV for all IJ solutions. IJ fiber production was verified for a wide range of applied voltage. When the electric potential was below 12 kV, all the IJ solutions produced very few fibers. IJ fiber production and deposition were dramatically improved for an applied voltage around 15kV. This bigger degree of attraction between the opposite charged fibers and grounded collector is a consequence of improved electric forces.

It was not found an upper voltage limit for the electrospinning of IJ solutions. When the electric potential surpassed 21 kV, the whole electrospinning setup began to suffer from high instability with spark formation around the capillary needle. For safety concerns, it was chosen not to surpass this limit for the electrospinning of IJ solutions.

3.3.3.3 Distance

Distance from the tip of the capillary needle and the grounded collector is another important parameter for electrospinning. Distance is inversely related to the electric field. Additionally, a distance increase allows the fiber to take more time to reach the grounded collector. When the fiber is forced to follow a bigger path on its way to the collector, the solvent

has more time to evaporate, allowing fiber thinning. If the distance between the needle and collector is too short the solvent will not have time to evaporate properly and, in some cases, beads and defects can be expected due to instability caused by high electric fields.

IJ electrospinning was possible for a wide range of capillary – collector distances. When the distance was kept below 10 cm it was difficult to obtain fibers and the fiber jet was remarkably instable. Fibers were also notoriously larger due to insufficient time for solvent evaporation. Fiber production yielded better results for distances between 14 and 20 cm. Distances greater than 20 cm resulted in a diminished fiber deposition on the collector. Fiber deposition, especially for distances above 15 cm, started to happen in the electric heater's grid, as demonstrated in **Figure 3.7**. For distances above 20 cm, there was more fiber deposition on the heater than the grounded collector. For this reason, it was chosen that, with this heating system, the distance from the capillary needle and the grounded collector should be between 15 and 20 cm.

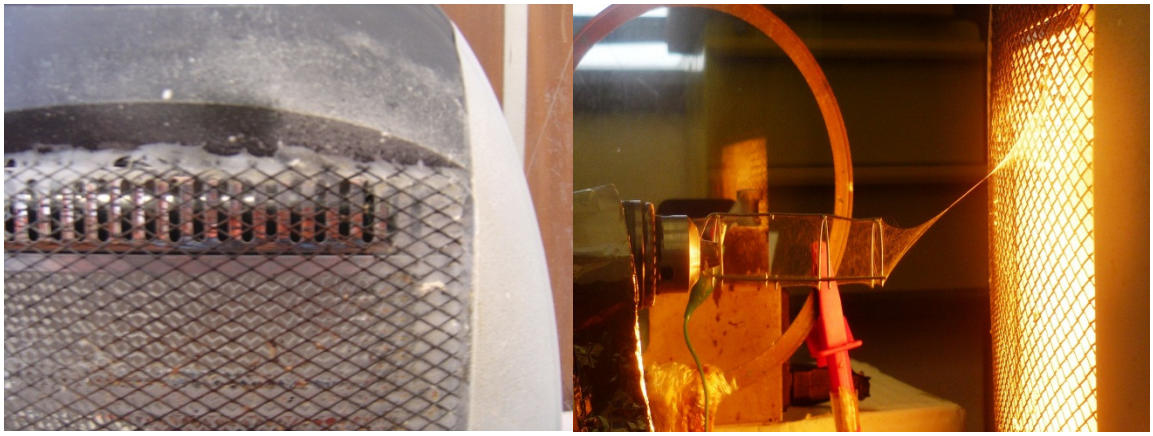

Figure 3.7 – IJ fiber deposition on the electric heater's grid.

3.3.3.4 Flow rate

Flow rate has an important effect on fiber production. During fiber production, the polymer solution flow rate must be high enough to stabilize the volume of the Taylor cone. Defects (like fiber fusion) and high fiber diameter can be a consequence of excessive flow rates. If a high amount of polymer solution is fed to the tip of the capillary needle, more polymer solution will be pushed out to the collector. This increase of the Taylor cone volume and fiber jet will difficult the evaporation process and fiber thinning.

Another aspect that needs to be taken into account is that the IJ electrospinning is temperature dependent because of gelatin melting point. Taylor cone gelification is a usual event for the electrospinning of IJ solutions. For this reason, the capillary needle needs to be clean in order to keep the fiber production running. The usual flow rates which minimized Taylor cone gelification were between 0,08 and 0,25 mL/h. Electrospinning of IJ – [Ch][Ti] generally needed higher flow rates than the other IJ solutions due to reduced viscosity.

3.3.3.5 Other parameters

Humidity also affects IJ fiber production through electrospinning. It was verified that when humidity values were above 30% fiber production was seriously affected. High percentages of water vapour in the atmosphere difficult solvent evaporation, fiber deposition and promote fiber fusion.

3.4 SEM

The IJ solutions described in **Table 3.5** were subjected to different electrospinning parameters during fiber production. The effect of applied voltage and distance from the capillary needle and collector on fiber diameters and morphology were analyzed. **Table 3.6** lists the average diameters of IJ fibers obtained for different electrospinning conditions.

Table 3.6 – Mean diameters (μm) of IJ electrospun fibers obtained and their variation with different electrospinning parameters.

		Distance (cm)			
		15		20	
Voltage (kV)		15	18	15	18
IJ	[Ch][Ac]	1,08 ± 0,25	0,99 ± 0,25	0,99 ± 0,23	1,03 ± 0,22
	[Ch][Ma]	1,06 ± 0,23	1,16 ± 0,19	1,04 ± 0,26	1,14 ± 0,27
	[Ch][Ti]	1,23 ± 0,33	1,17 ± 0,13	1,10 ± 0,41	1,16 ± 0,29
	[Ch][Ib]	0,96 ± 0,23	1,01 ± 0,21	0,88 ± 0,25	0,87 ± 0,14

Note: Fibers depicted in SEM images were measured using ImageJ® software.

According to **Table 3.6** choline based IJ fibers obtained through electrospinning have mean sizes around the lower end of the micrometer range. With the right combination, some sub-micrometer average values can be obtained too.

Table 3.6 puts in evidence that IJ – [Ch][Ib] fibers have generally lower diameters when compared with their counterparts. On the other end it is noticeable that, regardless the electrospinning processing parameters studied, IJ – [Ch][Ti] fibers exhibit higher mean values and a slight trend for wider diameter dispersions. Not surprisingly, these two IJ solutions are in opposite ends in terms of electric conductivity and their relative diameters (and related dispersion for IJ – [Ch][Ti]) reflect the already mentioned fiber fusion phenomena.

Overall it is noticeable that regardless the variations of electrospinning parameters the average fiber diameters do not change significantly. Considering this, it can be concluded that a

distance of 15 cm between the capillary needle and the collector is long enough for water evaporation to occur. There is not any advantage performing electrospinning of IJ at 20 cm because fiber production yield is lower (accumulation on heater's grid) and there is not any reduction in fiber size.

These results can be compared to those obtained by Pimenta *et* al. for the electrospinning of IJ fibers with $[C_2OHmim][BF_4]$ [119]. The IJ solutions used for electrospinning of IJ – $[C_2OHmim][BF_4]$ had higher conductivities than the ones described and used in this work (around 10^{-3} S cm^{-1}). Not surprisingly, the resulting fiber diameters were higher, ranging between 2,7 and 5,6 μm according to IL content [119]. These results clearly confirm the influence of IJ solution conductivity in the electrospinning process.

SEM images were also useful to morphologically characterize IJ fibers. **Figure 3.8** shows IJ –[Ch][Ma] electrospun fibers (15 kV, 15 cm, 0,10 mL/h) with sub-micrometer diameters. There is also fiber fusion evidence, especially in fiber intersections. This result opens the possibility of further reduction IL content in IJ solutions in order to decrease IJ solution conductivity and avoid fiber fusion phenomena. However this correlation between IL content and fiber fusion phenomena must be cautiously evaluated, especially with a IL containing API ions like IJ-[Ch][Ma]. If the IL content is too low, fibers can become thinner (GAS fibers diameter with 35 % w/v gelatin and no IL = 211 nm [118]) and fiber fusion less evident, but it can also impair the biological properties of electrospun fibers due to low API concentration and the possibility of practical applications.

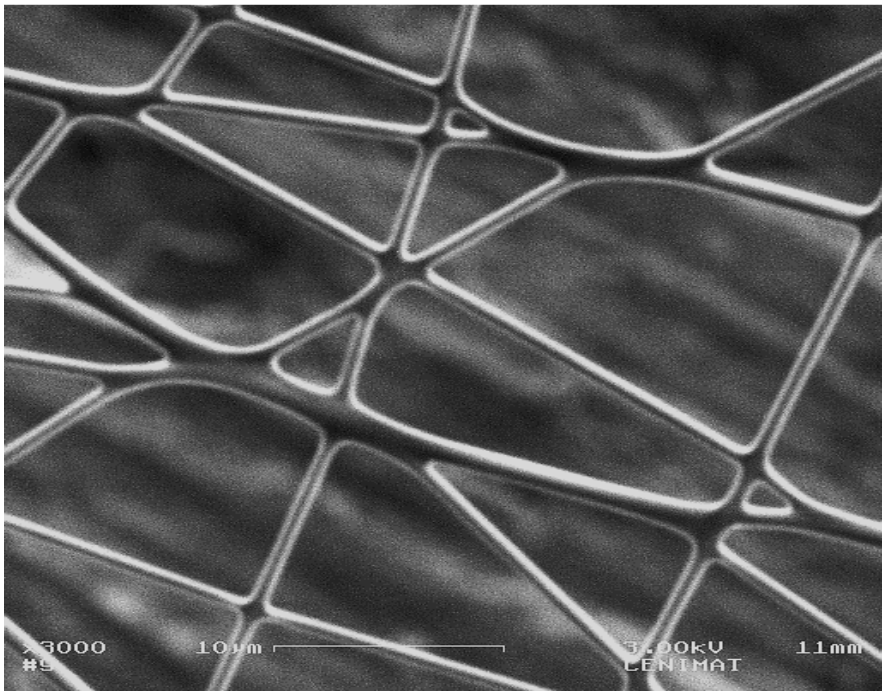

Figure 3.8 – SEM images of sub-micrometer IJ – [Ch][Ma] fibers (electrospun with an applied voltage of 15 kV, 15 cm distance and flow rate of 0,010 mL/h).

SEM images reveal that the electrospinning of choline-based IJ solutions described in **Table 3.5** yielded defect and bead-free fibers. According to **Figures 3.8, 3.9, 3.10 and 3.11**, electrospinning parameters do not have a significant effect of fiber morphology and diameters.

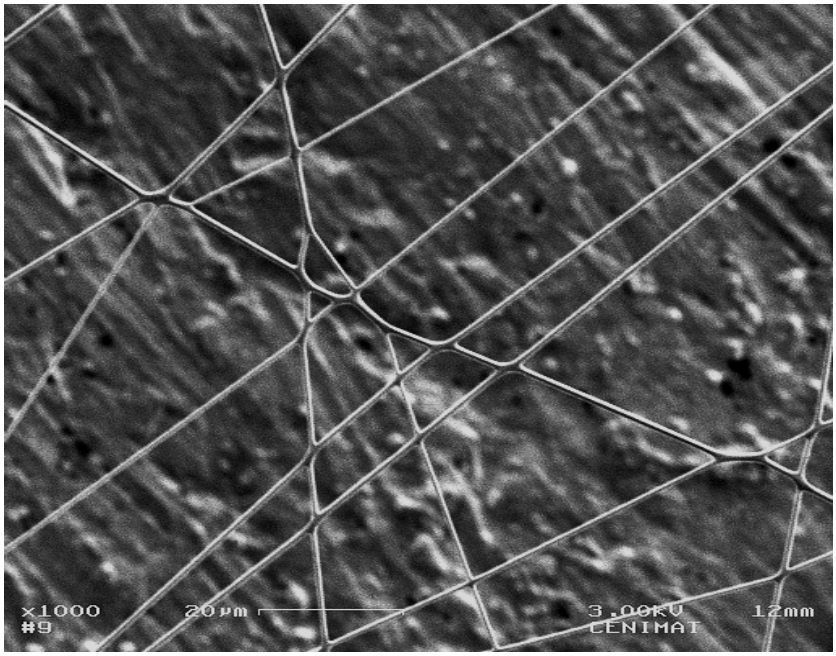

Figure 3.9 – SEM images of IJ – [Ch][Ti] electrospun fibers (electrospun with an applied voltage of 18 kV, 15 cm distance and flow rate of 0,025 mL/h).

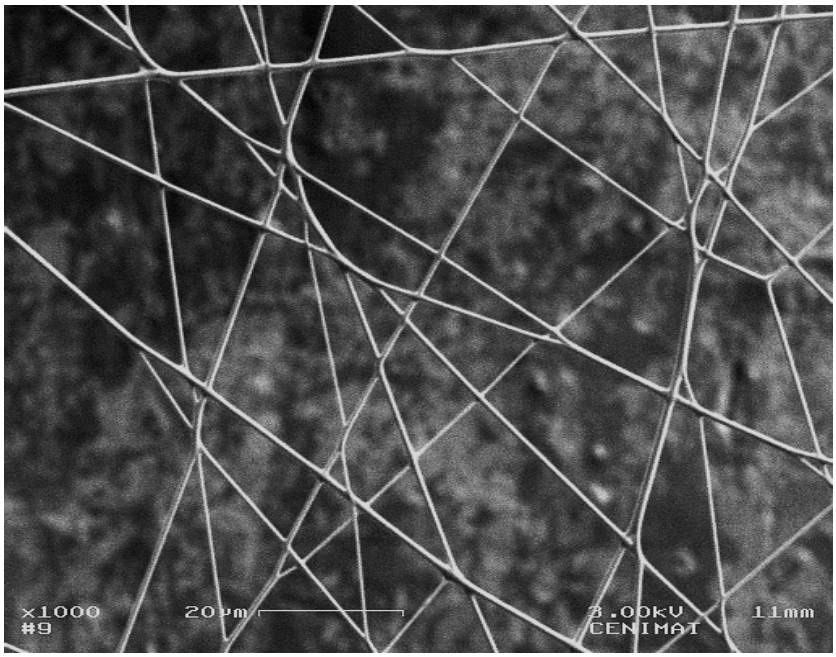

Figure 3.10 – SEM images of IJ – [Ch][Ib] electrospun fibers (electrotrospun with an applied voltage of 18 kV, 20 cm distance and flow rate of 0,010 mL/h.)

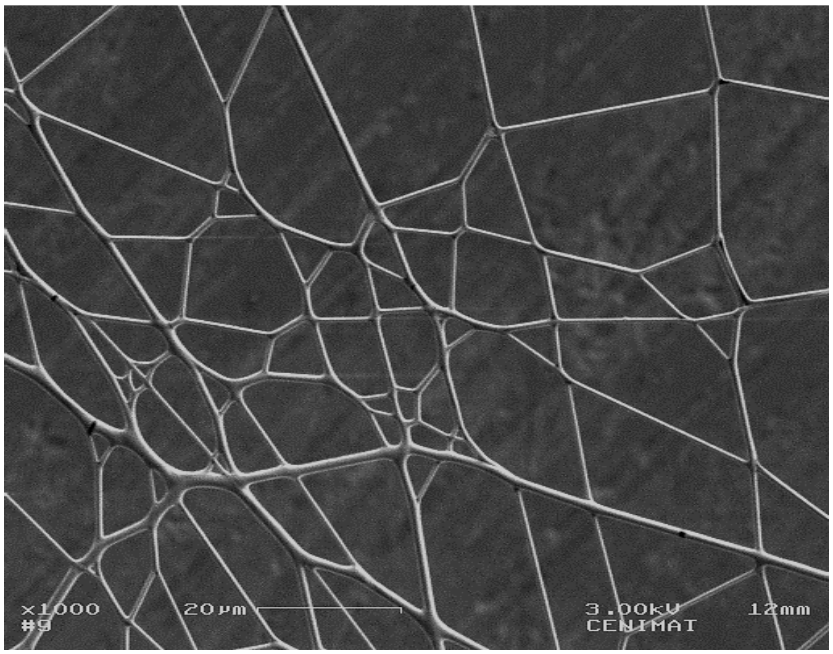

Figure 3.11- SEM images of IJ – [Ch][Ac] electrospun fibers (electrospun with an applied voltage of 15 kV, 20 cm distance and flow rate of 0,010 mL/h.)

3.5 IL – [Ch][Ma] quantification

The UV/Vis spectra for IL – [Ch][Ma] and the aqueous gelatin solution used as blanket are depicted in **Figure 3.12**.

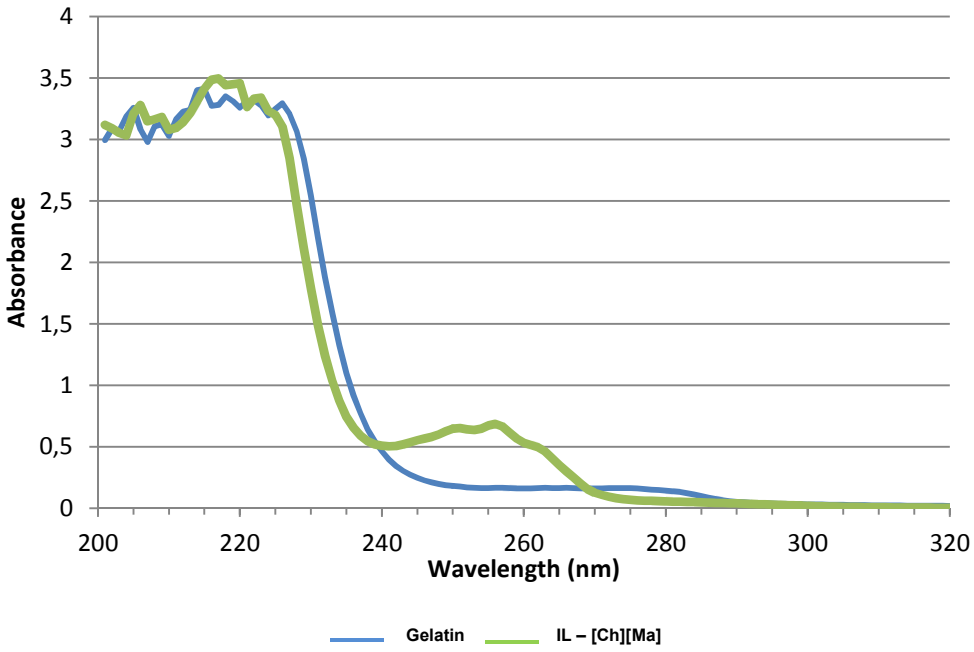

Figure 3.12 – UV/Vis spectra of IL – [Ch][Ma] and gelatin blanket.

Based on data from **Figure 3.12,** it is noticeable that IL – [Ch][Ma] has a maximum absorbance peak at 255 nm. In addition, gelatin reveals a relatively low absorbance in this spectra region. Therefore, 255 nm was the chosen working wavelength for the IL – [Ch][Ma] quantification in IJ – [Ch][Ma] fibers.

The calibration curve obtained is depicted in **Figure 3.13.**

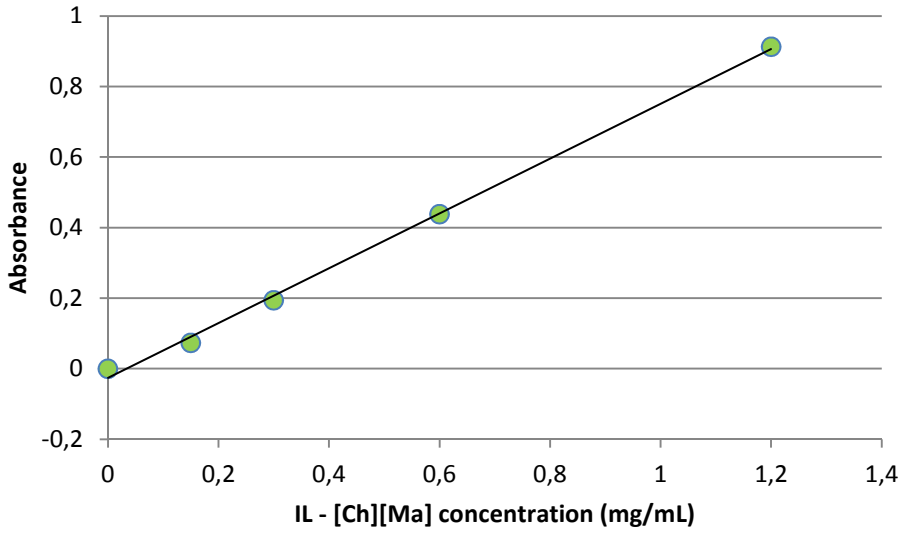

Figure 3.13 - Calibration curve for quantification of IL – [Ch][Ma] quantification in IJ – [Ch][Ma] fibers.*

Note: *- For this set of experimental points, the calibration curve is the following: $y = (0{,}7769 \pm 0{,}0651)x - (0{,}0258 \pm 0{,}0404)$ with an R^2= 0,9978.

The absorbance value for a sample of 4mg of IJ – [Ch][Ma], diluted in 5 mL of distilled water was A= 0,2540.

The obtained IL – [Ch][Ma] concentration in the IJ is 0,45 $\pm$ 0,04 mg / mg IJ fiber.

3.6 Antimicrobial activity

One of the aims of the present work was to evaluate if IL encapsulation in IJ electrospun fibers is an effective way of immobilization towards the efficacy improving of a given IL.

To evaluate that possibility the IL – [Ch][Ma] and IJ – [Ch][Ma] were selected for evaluation and comparison of their antimicrobial properties with mandelic acid. Mandelic acid and its derivates are well-known antibacterial agents. It is also a cosmetic peel with anti-aging effects in the same way as glycolic acid [128]. Diluted solutions of mandelic acid have been used

in some hospitals as bladder irrigation fluids to prevent urinary tract infections [129]. Urinary tract infections can be treated with the commercial drug Mandelamine (Park-Davis).

The first antimicrobial tests were performed to evaluate and compare the antimicrobial properties of mandelic acid with IL – [Ch][Ma] against the *E. coli* which is a gram-negative bacteria. In order to evaluate the best inoculum dilutions to work with, this test was carried out in two agar plates, one of them previously inoculated with 100 µL of undiluted pre-inoculum, described in section **2.1.9**. After inoculation, two paper disks containing the antibacterial agents mandelic acid and IL – [Ch][Ma] were put on each agar plates and the result is presented in **Figure 3.14**.

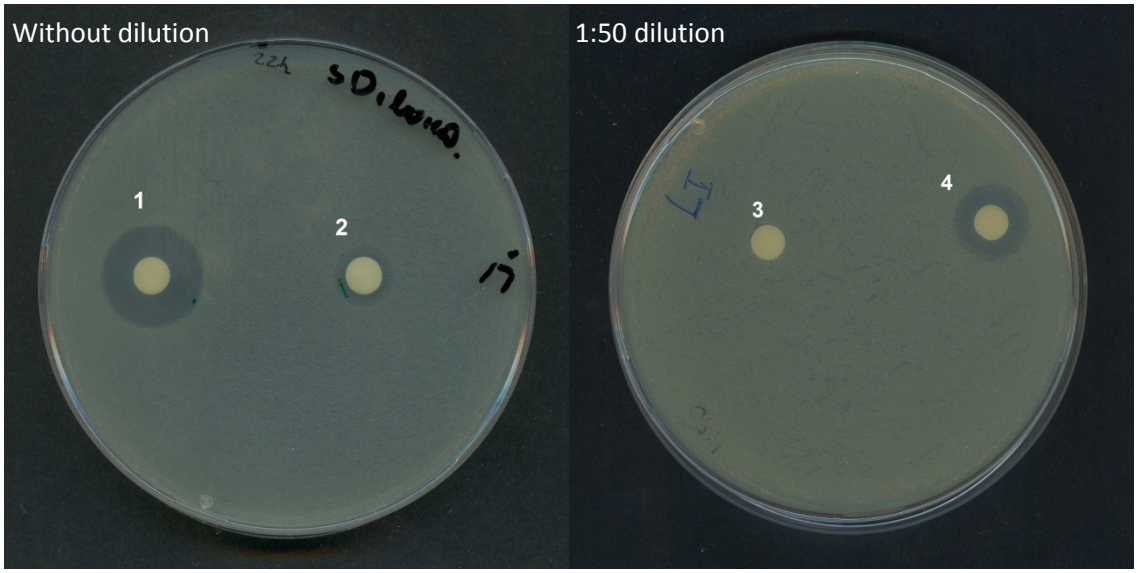

Figure 3.14 – Agar diffusion tests for mandelic acid and IL – [Ch][Ma] against *E. coli* (**1**- mandelic acid, **2, 3 -** IL – [Ch][Ma], **4-** mandelic acid).

The content of each paper disk is described in **Table 3.7**.

Table 3.7 – Content of the paper disks depicted in **Figure 3.7**.

Disk	V - Mandelic acid (µL)*	m Mandelic acid (mg)	IL – [Ch][Ma] (mg)	m Mandelate (mg)**
1	30	9,06 ± 0,03	-	-
2	-	-	15,6 ± 0,1	9,36 ± 0,06
3	-	-	11.5 ± 0,1	6,90 ± 0,06
4	20	6,04 ± 0,02	-	-

***Notes*: *** - Volume added from a (30,2 ± 0,1) x 10-2 mg/µL mandelic acid solution. **- Mandelate anion represents ≈ 60% of IL – [Ch][Ma]'s weight.

Figure 3.14 reveals that both mandelic acid and IL – [Ch][Ma] have inhibitory effect on *E. coli* 's growth. If fact our results are in agreement with the mandelic acid antimicrobial properties

described in literature [129], This result demonstrates that there is no loss of biological properties of the mandelate anion in the IL – [Ch][Ma]. This result suggests that there is a possibility that any API can be used as a part of an IL without compromising its properties.

One important result is the striking difference between the mandelic acid solution and IL – [Ch][Ma] in terms of antibacterial efficiency. As a matter of fact, aqueous mandelic acid solution outperforms its IL counterpart. This outcome is related not only with IL's viscosity and reduced diffusion in the paper disk matrix, but also with the reduced permeability of ILs in cell membranes compared to smaller compounds like mandelic acid.

Noteworthy is the result observed for disk **3** from the figure above. The most likely reason for the lack of inhibition is the addition of a smaller volume of IL on the disk. This smaller volume could not be high enough to allow the IL to reach and imbue the disk's edge, hampering even more the already difficult IL diffusion to the disk's surrounding zone. Insufficient IL concentration in the disk could also be admitted. However, it is needed to observe that disk **2** shows inhibition evidence. Despite being imbued with a higher IL volume, that agar plate has also a higher number of bacteria, given that it was inoculated with the undiluted pre-inoculum. The higher content of IL in the disk is counterbalanced with a higher bacteria density on the surrounding zone.

The next step in this work was the evaluation of IJ electrospun fibers as an effective way to overcome the IL diffusion problem and the related delivery of IL- [Ch][Ma].

After the evaluation and comparison of the antimicrobial properties of mandelic acid and IL – [Ch][Ma], the antimicrobial activity of IJ – [Ch][Ma] electrospun fibers was tested. A square of the metallic wire grid (area = 2 cm^2) used to collect the fibers was used directly in an agar plate inoculated with *E. coli.* The results are presented in **Figure 3.15**.

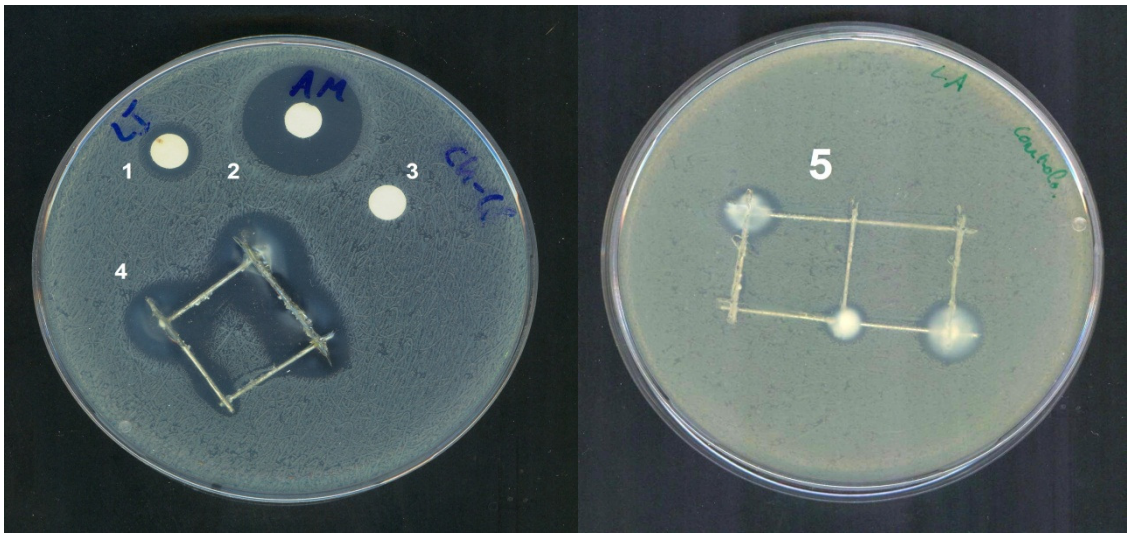

Figure 3.15 – Agar diffusion tests for IL – [Ch][Ma], mandelic acid, choline chloride, IJ – [Ch][Ma] and wire control against *E. coli* (**1**, IL- [Ch][Ma]; **2**, mandelic acid; **3**, Choline chloride; **4**, IJ – [Ch][Ma] fibers supported in the wire grid collector; **5**, wire control).

The content of each paper disk and the wire grid square is described in **Table 3.8**.

Table 3.8 – Content of the paper disks and wire grid square depicted in **Figure 3.15**.

Disk / wire grid square	Content	Mass or volume	m mandelic acid (mg)	m mandelate (mg)****
1	IL – [Ch][Ma]	(15,1 ± 0,1) mg	-	9,06 ± 0,06
2	Mandelic acid	30 µL*	9,06 ± 0,03	-
3	Choline chloride	10 µL **	-	-
4	IJ – [Ch][Ma] fibers***	(20,9 ± 0,1) mg	-	5,65 ± 0,04*****
5	Wire grid control	-	-	-

Notes: * - Volume added from a (30,2 ± 0,1) x 10^{-2} mg/µL mandelic acid solution. ** – Volume added from a (0,60 ± 0,01) mg / µL choline chloride solution. *** – Fibers electrospun with IL concentration 23% v/v, 15kV, 15 cm and 0,010 mL/h. **** - Mandelate anion represents ≈ 60% of IL – [Ch][Ma]'s weight. ***** – Mandelate mass present in (9,41 ± 0,07) mg of IL-[Ch][Ma].

Figure 3.15 presented in previous page shows that IJ – [Ch][Ma] fibers do inhibit *E. coli*'s growth, despite fiber accumulation on the square lateral parts. This accumulation left a zone right inside the square where there was no growth inhibition owing to the absence of fibers.

Despite the evidence of the fiber's antimicrobial activity, unfortunately their real efficiency cannot be evaluated due to interference of the wire grid collector. The wire grid also inhibits bacterial growth and this fact is particularly visible at the grid's joints (**5**). At those spots there is a presence of a whitish area surrounded by a bacteria free zone. The hypothesis of fungal contamination was abandoned because the wire grid was sterilized prior to use and further inoculation of the white spots did not reveal any microorganism. The humid sterilization process or even the moisture present in the agar plate could have triggered the wire's oxidation process. It is known that some metal oxides inhibit bacterial growth and this particular feature have rendered them a growing interest for applications as antibacterial agents in nanotechnology [130]. As expected, choline chloride does not inhibit bacterial growth.

Despite the results obtained, further experiments were carried out to evaluate the efficiency of the IJ – [Ch][Ma] electrospun fibers without the interference of the wire grid collector. To avoid the wire grid oxidation in moisture or during humid sterilization, a stainless steel wire was used as a carrier for the fibers positioned in the wire grid collector. After fiber production through normal conditions, fibers were transferred to the stainless steel square. The results of this test are depicted in **Figure 3.16**.

Figure 3.16 - Agar diffusion tests for IJ – [Ch][Ma], mandelic acid, IL – [Ch][Ma] on stainless steel wire and wire control against *E. coli* (**1**, IJ – [Ch][Ma] fibers; **2**, Mandelic acid; **3**, IL – [Ch][Ma]; **4**, wire control).

The content of each paper disk and wire specifications is described in **Table 3.9**.

Table 3.9 – Content of the paper disks and wire grid square depicted in **Figure 3.16.**

Disk / wire	Content	Mass or volume	m mandelic acid (mg)	m mandelate (mg)***
1	IJ – [Ch][Ma] fibers*	(37,8 ± 0,1) mg	-	10,21 ± 0,91****
2	Mandelic acid	30 µL **	9,06 ± 0,03	-
3	IL – [Ch][Ma]	(14,9 ± 0,1) mg	-	8,94 ± 0,06
4	Wire control	-	-	-

Notes*:** * - Fibers electrospun with IL concentration 23% v/v, 15kV, 15 cm and 0,010 mL/h. ** – Volume added from a (30,0 ± 0,1) x 10^{-2} mg/µL mandelic acid solution. *** - Mandelate anion represents ≈ 60% of IL – [Ch][Ma]'s weight. * - Mandelate mass present in (17,01 ± 1,51) mg of IL-[Ch][Ma].

With the use of the stainless steel wire it is possible to truly evaluate the antimicrobial activity of IJ – [Ch][Ma] fibers against *E. coli*. The wire control (**4**) did not inhibit bacterial growth. One important result is the reduced inhibition presented by the mandelic acid control (**2**). After the agar plate overnight incubation it was verified that mandelic acid was not entirely solubilized and crystallization did occur. This is an interesting result which means that mandelic acid can have solubility and polymorphism limitations that can affect its antibacterial efficiency.

The IJ fibers presented fairly good results. Wire **1** successfully inhibited bacterial growth without membrane rupture. This improved mechanical resistance can be related to a higher fiber density on the new membrane compared to the previously tested (**Figure 3.16 – 4**). Wire **1**

not only has a lower area (1 cm^2) compared to wire **4** showed on **Figure 3.15,** but also has higher fiber mass due to increased time of fiber deposition. These two factors contribute to improve mechanical resistance.

Data presented in **Table 3.10**, shows that wire **1** content inhibited *E. coli*'s growth in a much more efficient way than disk **3**. The IL encapsulated in IJ electrospun fibers outperforms the unencapsulated IL. The ratio between inhibition area and mandelate anion / IL content is more favorable for the IJ fibers because the IL encapsulated in the IJ electrospun matrix has bigger ratio surface / volume. The same amount of IL can be released in a more efficient way because the improved surface area facilitates the IL diffusion on the agar and the consequent access to bacterial membranes.

Table 3.10 - Antibacterial efficacy of mandelic acid, IL-[Ch][Ma] and IJ-[Ch][Ma] fibers against *E. coli*.

Disk / wire	Content	Inhibition area (cm^2)*	m Antibacterial agent (mg)**	Ratio area / m Antibacterial agent (cm^2/mg)
1	IJ – [Ch][Ma] fibers	2,29	10,21 ± 0,91	(23,14 ± 2,05) x 10^{-2}
2	Mandelic acid	1,41	9,06 ± 0,03	(15,60 ± 0,05) x 10^{-2}
3	IL – [Ch][Ma]	0,55	8,94 ± 0,06	(6,20 ± 0,04) x 10^{-2}

Notes*: * -** Areas were calculated through analysis of **Figure 3.16** , using ImageJ® software for measures. Paper disk radius = 0,6 cm and wire **1** side = 1 cm. * -** Mandelate anion represents ≈ 60% of IL – [Ch][Ma]'s weight.

According to data shown in **Table 3.10**, there is an almost fourfold increase of IL antimicrobial activity efficiency after encapsulation in electrospun IJ fibers. The increased surface volume reduces the problem of slow IL diffusion and viscosity, allowing the IL to be even more effective as the API mandelic acid regarding inhibition growth of *E. coli*.

Antimicrobial activities of mandelic acid, IL - [Ch][Ma] and IJ – [Ch][Ma] were also tested against Gram-positive bacteria *B. subtilis*. The same procedure for *E. coli* was adopted. To avoid wire collector oxidation interference, IJ fibers were first tested in a squared-shaped stainless steel support (area = 1 cm^2).

The results and test specification are shown in **Figure 3.17** and **Table 3.11,** respectively.

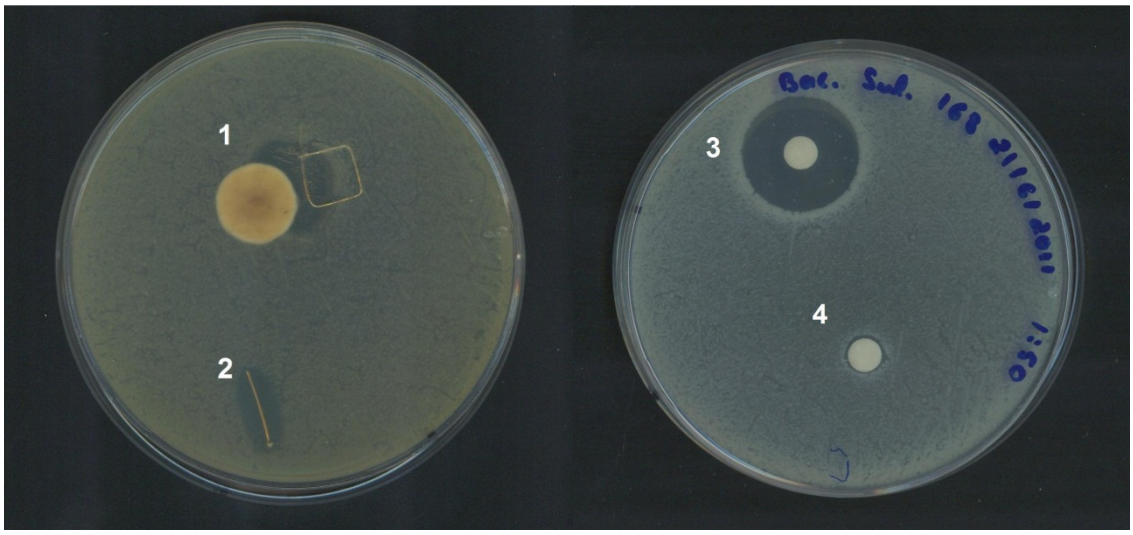

Figure 3.17 - Agar diffusion tests for mandelic acid, IL – [Ch][Ma], IJ – [Ch][Ma] on stainless steel wire and wire control against *B. subtilis* (**1**, IJ – [Ch][Ma] fibers, **2**, wire control; **3**, mandelic acid; **4**, IL – [Ch][Ma]).

Table 3.11 – Content of the paper disks and wire grid square depicted in **Figure 3.17**.

Disk / wire	Content	Mass or volume	m mandelate (mg)	m mandelate (mg)***
1	IJ – [Ch][Ma] fibers*	(29,8 ± 0,1) mg	-	8,05 ± 0,71
2	Wire control	-	-	-
3	Mandelic acid	30 µL **	9,06 ± 0,03	-
4	IL – [Ch][Ma]	(14,8 ± 0,1) mg	-	8,88 ± 0,06

Notes*:** * - Fibers electrospun with IL concentration 23% v/v, 15kV, 15 cm and 0,010 mL/h. ** – Volume added from a (30,2 ± 0,1) x 10^{-2} mg/µL mandelic acid solution. *** - Mandelate anion represents ≈ 60% of IL – [Ch][Ma]'s weight. * - Mandelate mass present in (13,41 ± 1,19) mg of IL-[Ch][Ma].

The results show that mandelic acid and IL – [Ch][Ma] have antimicrobial properties against *B. subtilis.* Not surprisingly, proof that mandelate's biological properties are diminished by the high viscosity and low diffusion of the IL arises again. The inhibition area for the IL – [Ch][Ma] is much lower than the area obtained with an equivalent amount of aqueous mandelic acid.

Unlike *E. coli's* case, *B. subtilis'* growth was surprisingly inhibited by stainless steel as demonstrated by the wire control. This unexpected result forced the search for a new fiber and inert carrier. It is visible, also, that contamination took place on the wire containing the IJ – [Ch][Ma] fibers by bacteria that are resistant to mandelic acid or IL – [Ma][Ch].

The non-conductive plastic grid previously tested for the electrospinning optimization was the chosen alternative to function as fiber carrier. After fiber collection on a plastic square, which

was performed in the same way as stainless steel carriers previously described, a new test was carried out and the results and specifications are presented below (**Figure 3.18** and **Table 3.12**).

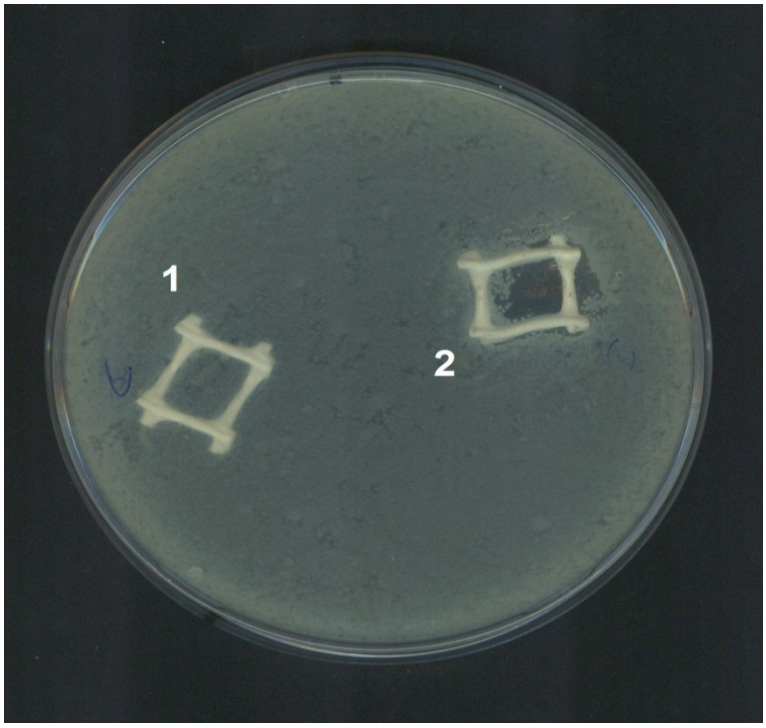

Figure 3.18 - Agar diffusion tests for IJ – [Ch][Ma] fibers supported on a plastic carrier and plastic control against *B. subtilis* (**1**, plastic control; **2**, IJ – [Ch][Ma] fibers).

Table 3.12 – Content of plastic carriers depicted in **Figure 3.18**.

Plastic square	Content	Mass or volume	m Mandelate (mg)**
1	Plastic control	-	-
2	IJ – [Ch][Ma] fibers*	(30,7 ± 0,1) mg	8,29 ± 0,74

***Notes*:** * - Fibers electrospun with IL concentration 23% v/v, 15kV, 15 cm and 0,010 mL/h. **- Mandelate mass present in (13,82 ± 1,23) mg of IL-[Ch][Ma].

Without the interference of the plastic fiber carrier it is possible to evaluate the antimicrobial activity of IJ – [Ch][Ma] fibers against *B. subtilis*. The fibers did inhibit bacterial growth without membrane disruption (**Figure 3.18 - 2**).

Data shown in **Table 3.13** demonstrate how IJ – [Ch][Ma] fibers enhance the antimicrobial properties of IL – [Ch][Ma] against *B. subtilis.* These results reinforce that the encapsulation of IL in IJ fibers produced through electrospinning can be considered an effective way of improving ILs properties. The biological properties of IL – [Ch][Ma] are enhanced by a larger surface area which benefits diffusion and attenuates mass transport problems caused by high viscosity.

Table 3.13 - Antibacterial efficacy of mandelic acid, IL-[Ch][Ma] and IJ-[Ch][Ma] fibers against *B. subtilis*.

Disk / wire	Content	Inhibition area (cm^2)*	m Antibacterial agent (mg)**	Ratio area / m Antibacterial agent (cm^2/mg)
2	IJ – [Ch][Ma] fibers	1,06	8,29 ± 0,74	(12,80 ± 1,14) x 10^{-2}
3	Mandelic acid	3,46	9,06 ± 0,03	(38,20 ± 0,13) x 10^{-2}
4	IL – [Ch][Ma]	0,39	8,88 ± 0,06	(4,40 ± 0,03) x 10^{-2}

***Notes*: * -** Areas were calculated through analysis of **Figure 3.17** and **Figure 3.18**, using ImageJ® software for measures. Paper disk radius = 0,6 cm and plastic square side = 1 cm. ** **-** Mandelate anion represents ≈ 60% of IL – [Ch][Ma]'s weight.

For *B. subtilis*, IL – [Ch][Ma] encapsulation of IL in a IJ porous fiber membrane almost tripled its antimicrobial efficiency. Even though IJ – [Ch][Ma] fiber membranes enhanced the IL properties, for *B. subtilis* mandelic aqueous solutions provide better results, in opposition with the results obtained with *E. coli* cultures. For the latter case mandelic acid had solubilization problems which also contribute for the obtained results and the better performance of IJ – [Ch][Ma] compared to mandelic acid. **Figure 3.17** demonstrates that if solubilization problems are absent, mandelic acid outperforms its counterparts, because of higher diffusion rate, easier cell membrane penetration and diminished viscosity.

The results also suggest that *B. subtilis* is less sensitive to IL – [Ch][Ma] and IJ – [Ch][Ma] than *E. coli*. Not surprisingly, the former have generally lower ratios area / mass of antibacterial agent, meaning that for nearly the same quantity of antibacterial agent, the inhibition area is smaller. As Gram-positive bacteria, *B. subtilis is* possibly more resistant to these antibacterials owing to the higher amount of peptidoglycan on the cell wall.

Considering all the concerns about ILs toxicity, the success and practical applicability of any IL-API drug delivery system their practical applicability is dependent on toxicity assessment. In collaboration with Dr Ana Nunes and Dr Catarina Duarte from IBET, the toxicity of all choline based ILs used in this work was evaluated. The results showed that all choline-based ILs described and used in this work were non-toxic to CaCo-2 cells, with the unsurprising exception of IL – [Ch][Ib]. In fact, ibuprofene toxicity is a well and long-known feature [131]. Apparently, ibuprofen toxicity is not higher when being part of an IL-API.

These results are a positive sign towards practical applications of IL-APIs. ILs-APIs can also be considered non-toxic or not more dangerous than other crystalline APIs in the market. With a wise ions choice, IL-APIs can be considered safe and their encapsulation in IJ fibers produced through electrospinning can create a really successful drug delivery system.

3.7 Tensile tests

The IJ solutions used to prepare dense membranes were the same used for fiber production through electrospinning (**Table 3.3**).

The results of tensile test for IJ – [Ch][Ac], IJ – [Ch][Ma], IJ – [Ch][Ti] are presented in **Figure 3.19**. For IJ – [Ch][Ib], tensile test data are presented in **Figure 3.20**.

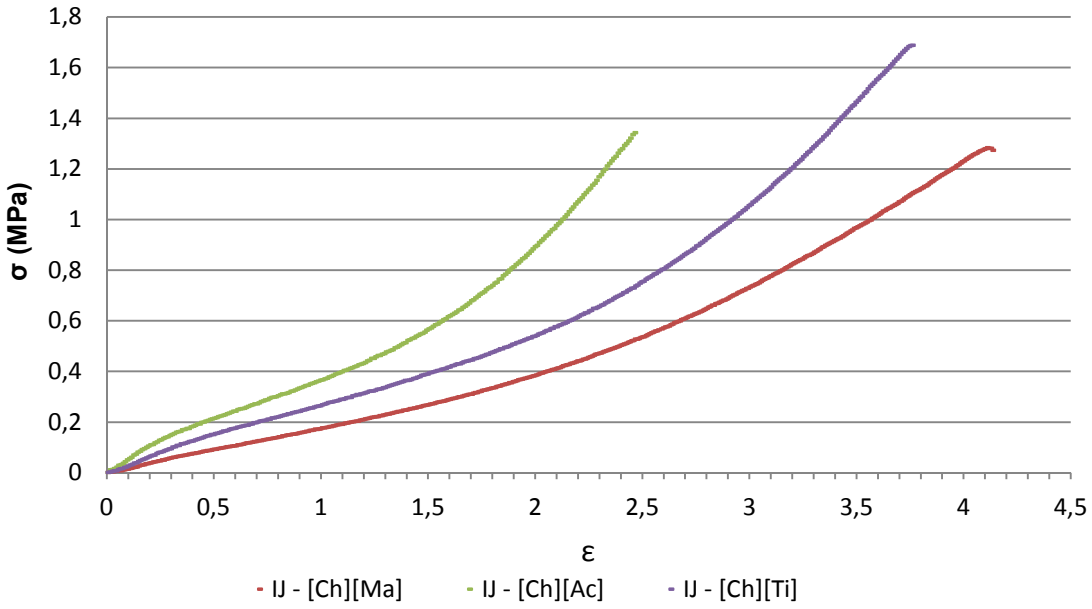

Figure 3.19 - Stress (σ) – strain (ε) curves of IJ – [Ch][Ac], IJ – [Ch][Ma], IJ – [Ch][Ti] dense films.

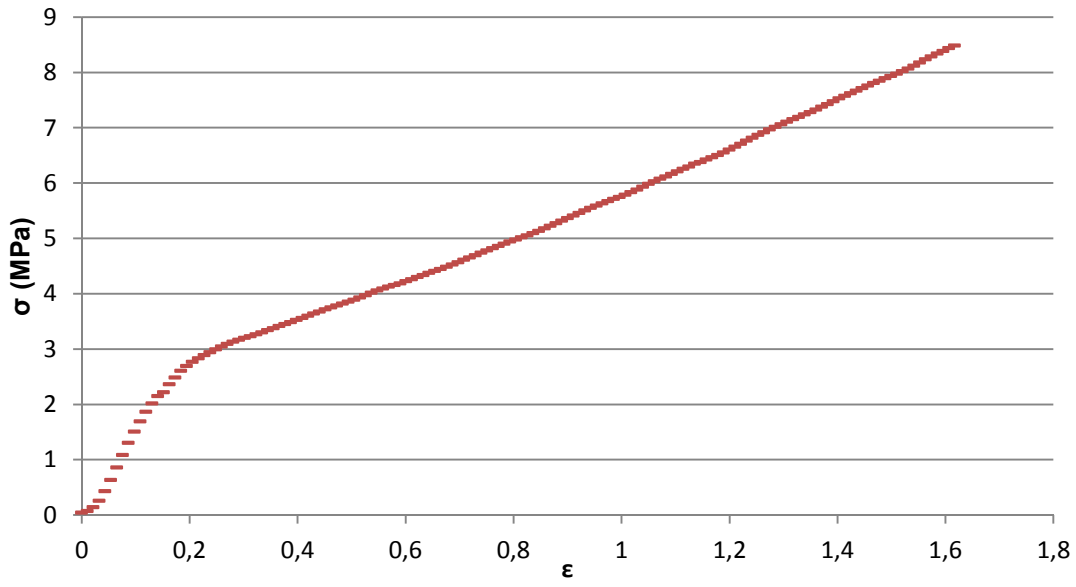

Figure 3.20 - Stress (σ) – strain (ε) of IJ – [Ch][Ib] dense film.

Table 3.14 summarizes some mechanical data of IJs dense membranes taken out from tensile tests.

Table 3.14 - Mechanical properties of choline-based IJs.

IJ*	Stress at break, σ_b (Mpa)	Strain at break ε_b	Young's modulus, E (MPa)	Shear modulus, G (MPa)
IJ – [Ch][Ac]	1,34	2,46	0,56 ± 0,02	0,18 ± 0,02
IJ – [Ch][Ma]	1,27	4,13	0,14 ± 0,02	0,05 ± 0,01
IJ – [Ch][Ti]	1,69	3,76	0,24 ± 0,03	0,09 ± 0,01
IJ – [Ch][Ib]	8,49	1,62	19,60 ± 0,65	-

***Notes* :** *- thickness values in mm: IJ- [Ch][Ac] = 0,11 ± 0,01. IJ- [Ch][Ma] = 0,18 ± 0,01. IJ- [Ch][Ti] = 0,14 ± 0,01. IJ – [Ch][Ib] = 0,23 ± 0,02.

The stress-strain curves observed for IJ – [Ch][Ac], IJ – [Ch][Ma] and IJ – [Ch][Ti] dense membranes unveil a typical mechanical behavior of an elastomer in temperatures above T_g. Elastomers are well-known for their high yield strains and large, non-linear elastic behavior when subjected to low stresses. This mechanical behavior is caused by elastomer structure with long polymer cross-linking chains. Elastomers elasticity is affected by cross-linking degree.

At low elongations the curve is linear and Hooke's law is valid. With further stretching, the stress – strain curve slope gradually changes to lower values, meaning that the membranes' stiffness is reduced. This is caused by the polymer chain uncoiling, demonstrated in **Figure 3.21**.

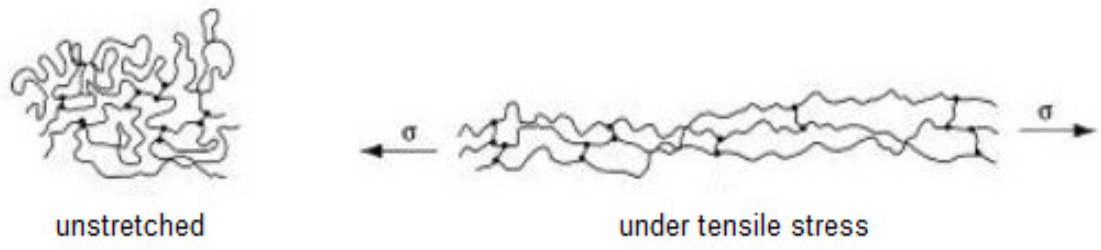

Figure 3.21 – Effect of tensile stress on elastomer structure [132].

Uncoiling enables conformational changes and the possibility of stress redistribution in the polymer structure. It is noticeable that after uncoiling, further stretching will lead to stiffness increase. With the polymer chains uncoiled, chemical bonds and cross-linking points begin to be subjected to stress. This explains the higher curve slopes at higher elongations.

Strain at break (ε_b) is higher for these elastomeric materials and IJ – [Ch][Ma] exhibits the biggest value, nearly followed by IJ – [Ch][Ti]. Stress at break values are equal to ultimate tensile strengths and, for the elastomeric-like IJs, their values are between 1,27 and 1,69 MPa.

The Young's modulus for an elastomer can be obtained from the curve slope at very low deformations, where linearity is observed and Hooke's law is valid. Values are presented in **Table 3.14.** Elastomers usually have low Young's modulus values, and the lowest is (0,14 ± 0,02) MPa for IJ – [Ch][Ma].

For low deformations the rubber Young's modulus and shear modulus can be related by E = 3G. In uniaxial tensile tests it can be admitted that the tensile force is the only force being exerted on the IJ dense membrane and has the direction of extension. According to the statistical theory of rubber elasticity, the shear rubber modulus is given by: $\sigma = G (\lambda - 1/\lambda^2)$, where σ is the stress and λ is the extension ratio ($\lambda = l / L_0$, l = length, L_0 = initial length) [133]. This ratio is observed for IJ – [Ch][Ac], IJ – [Ch][Ma] and IJ – [Ch][Ti] (**Table 3.14)**.

The stress-strain curves obtained for IJ dense membranes reveal that IJ-[Ch][Ib] has, once more, a completely distinct behavior and set of mechanical properties compared to other IJs studied. The IJ – [Ch][Ib] stress-strain curve puts in evidence that this IJ does not have elastomer-like properties. The curve shows that IJ – [Ch][Ib] exhibits higher brittleness and more limited deformation ability. It is worth noting that this IJ membrane is also a much stronger material than its IJ counterparts. Stress at break is also about eight times higher while strain at break is lower than the rest of the other IJs.

In order to understand the mechanical distinctive behavior of IJ – [Ch][Ib], water content in all IJ dense membranes tested were determined by KF titration. The results are presented in **Table 3.15**:

Table 3.15 – Water content in IJ dense films determined by KF titration at room temperature.

IJ	Water content (mg_{H2O} / g_{IJ})
IJ – [Ch][Ac]	**220,178** ± 15,7
IJ – [Ch][Ma]	**248,3** ± 13,9
IJ – [Ch][Ti]	**273.3** ± 19,4
IJ – [Ch][Ib]	**180,5** ± 18,7

Data from **Table 3.15** show that IJs with elastomeric mechanical behavior have higher water content than the brittle and stiff IJ – [Ch][Ib]. For the former three IJs, water content is within the same order of magnitude. Additionally, IJ – [Ch][Ib] has a lower water content which can reflect and justify the distinct behavior. Zhang *et* al. observed that water presence in porous gelatin films cross-linked with carbodiimide hydrochloride resulted in a modified mechanical behavior [118]. Water presence lowered Young's modulus and led to an increase of elasticity. Taking this into account, water must have an important role on gelatin chains mobility, allowing higher conformational freedom and consequent elasticity.

4 ELECTROSPINNING OF OTHER BIOPOLYMERS

DNA and dimehtylchitosan were used as substitutes of gelatin for the preparation of polymer solutions with IL suitable for fiber production through electrospinning.

4.1 DNA

DNA, the carrier of genetic information, can also be seen as a polymer. DNA application in materials science as a polymer is very limited. In a recent literature review, there are only three cases reporting the successful electrospinning of DNA. In 1997, Fang and Reneker electrospun DNA fibers with 50 to 80 nm of diameter from 0,3 – 1,5 % w/v Calf Thymus DNA solutions in a 7:3 water/ethanol mixture [134]. Similar outcomes were obtained by Takahashi *et* al. with DNA fibers electrospun from a 1,5 % w/v DNA solution using a 7:3 water/ethanol mixture as solvent [135]. DNA blended with PEO yielded fibers between 50 and 250 nm from aqueous solutions [136].

Salmon milt DNA solutions, with concentrations ranging from 0,5 up to 40% w/v, were prepared for electrospinning in the same way described by Fang and Reneker [134]. No fibers were produced and even in the most concentrated solutions, electrospraying did occur. This lack of fiber entanglement and droplet production even with high concentrations can be related with the low molecular weight of salmon milt DNA. Cal thymus DNA used by Reneker was claimed to have a molecular weight of 10^9 g/mol whilst DNA extracted from salmon testes is about 10^6 [137].

Taking into account the importance of polymer molecular weight for electrospinning, Calf Thymus DNA solutions with DNA concentration up to 5% were prepared. Despite the increase of molecular weight, the results obtained by Fang and Reneker were not reproducible.

Several parameters were tested in order to evaluate the electrospinning of DNA. Wallace *et* al. verified that electrospinning of DNA in water did not produce fibers [136]. It becomes clear then that ethanol played an important role of raising volatility and eased the electrospinning evaporation process in Reneker's procedure [134]. Despite this advantage regarding ethanol usage for electrospinning, DNA solubility is severely affected in the presence of alcohols.

These two facts create a difficult correlation between polymer solubility and solvent evaporation for electrospinning of DNA. If the alcohol content in the solvent mixture is raised, DNA solubility is accordingly lowered, resulting in a lack of polymer concentration that hampers fiber production and entanglement. On the other hand there is evidence that for achieving successful fiber production the solvent must be more volatile than water, which implies the addition of an organic compound that will limit DNA solubility and correlated fiber production.

In order to avoid this quandary, DNA aqueous solutions with ILs were prepared and used as solvents for electrospinning. Two ILs were tested for DNA solubilization and electrospinning parameter evaluation, namely [C_2OHmim][BF_4] and [bmim][Cl]. The latter is well known for solubilizing cellulose [30].

DNA did not solubilize in the presence of [C_2OHmim][BF_4]. DNA aqueous solutions with concentrations ranging from 0,5 up to 3% w/v in an 7:3 water/[bmim][Cl] solution were put in the electrospinning setup.

The solutions presented high viscosity and heating was needed to prevent gelification for DNA concentration above 1,5 %w/v, just like IJ solutions. Taylor cone is observed around 12,5 kV and voltage increase leads to electrospraying and droplet formation. Despite the impossibility of producing proper DNA fibers, electrospinning of a 3% w/v DNA solution in 7:3 water/[bmim][Cl] solution was almost achieved with an applied voltage of 15 kV, a distance from the capillary needle to an aluminium plate of 14 cm and a flow rate of 0,01 mL / h.

Among the droplets some fiber jets were observed, putting in evidence an attempt of fiber production. However, both droplets and fibers were wet. Notwithstanding the ability of [bmim][Cl] aqueous solutions to dissolve DNA, the addition of IL to the solvent lowers its volatility and impairs fiber production and thinning.

This attempt of fiber formation is a good preliminary result that encourages the study of IL influence on other biopolymers beyond gelatin. Combination and synthesis of different ILs, optimization of solution concentrations for the electrospinning process can constitute a brand new challenge to be taken on a different context and time.

4.2 Dimethylchitosan

Chitosan is the N-deacetylated derivative of chitin, the second most abundant biopolymer after cellulose [113]. Chitosan and its derivates are well-known for a vast range of properties such as biocompatibility and antibacterial activity [138].

Chitosan is a difficult biopolymer to be electrospun because it has a high degree of strong hydrogen bonds between its molecules. Acid aqueous solutions with organic acids enables chitosan solubilization owing to the protonation of the $–NH_2$ group of the glucosamine monomers. Dilute acetic acid, formic acid and malic acid solutions are usually used to solubilize chitosan [113]. Reports claiming chitosan electrospinning are usually performed with aqueous organic acid solutions (acetic acid, mainly) and chitosan blended with other polymers such as PVA and PEO.

N,N-dimethylchitosan was tested for electrospinning with IL. The $–NH_2$ group modification of the glucosamine monomers to a $–N(CH_3)_2$ lowers the intensity of hydrogen bonding between

polymer chains. This modification can open up to a vast range of solubilization possibilities and ease electrospinning of chitosan.

Up to this point, this polymer could not be solubilized in any IL. N,N-dimethylchitosan was tested for electrospinning in strong acetic acid solutions (80% or more) in similar ways to other electrospinning reports for regular chitosan. However, the acetic acid solutions tested seemed to be too strong for a mild dissolution of this new polymer.

Like DNA, electrospinning of N,N-dimehtylchitosan has the potential to be explored in combination with other ILs or, in a preliminary phase, without them. Taking into account that its hydrogen bonds may have striking different patterns when compared with regular chitosan, it is necessary to better understand its properties. All this work needs to be done in order to have a clue of possible solvents that can be used its successful electrospinning of N,N-dimethylchitosan.

5 CONCLUSIONS

The development of ILs based on API ions is on the rise because of their tunable properties and the possibility of avoiding relevant problems for the pharmaceutical industry like polymorphism.

In this work, the development of a novel drug-delivery system based on IJ fibers produced through electrospinning was achieved. Encapsulation of IL in IJ fibers is an effective way to enhance the IL properties and avoid critical problems of ILs such as high viscosity and low diffusion rate.

Fiber production was optimized and the influence of IL on fiber morphology was studied through OM and SEM images. IL concentration and fiber diameters are positively correlated owing to high conductivity and impaired solvent evaporation. High IL content in the polymer solution modifies the charge distribution on fibers' surface. Fiber fusion is a consequence of attraction between fiber segments oppositely charged. Additionally, impaired evaporation needed for fiber thinning is also hampered because of the reduced volatility of ILs, contributing for higher diameters.

According to SEM images, IJ fibers were produced without beads and other defects, apart from a persistent fusion phenomena caused by IL high conductivity. Moreover, it was also verified that the variation of electrospinning parameters like distance from capillary needle to the grounded collector and applied voltage did not have significant influence on fiber morphology and respective diameters. In fact, fiber morphology was much more dependent on the type of IL used and its relative concentration. Despite the high degree of morphological similarity between the all IJ fibers produced, it should be noted that IJ-[Ch][Ib] fibers are slightly thinner than their counterparts. On the other hand, IJ-[Ch][Ti] fibers are usually thickest ones.

Antimicrobial assays put in evidence the sharp increase of antibacterial activity of IL – [Ch][Ma] when encapsulated in IJ. In some cases, antibacterial activity of IJ-[Ch][Ma] can be even superior than mandelic acid's. The biological properties of IL – [Ch][Ma] are enhanced by a larger surface area which benefits diffusion and attenuates mass transport problems caused by high viscosity. The potential of IJ fibers for the development of LI-API drug delivery systems was demonstrated.

Toxicity data was also obtained for all choline-based ILs used in this work. IL – [Ch][Ib] was the only IL that showed significant toxicity which agrees with the toxicity presented by the crystalline commercialized API ibuprofen.

Mechanical characterization of IJ dense films was also performed through uniaxial tensile tests. All IJs with the exception of IJ-[Ch][Ib] presented a typical elastomeric behavior. IJ –

[Ch][Ib], on the other hand, was found to be a much more brittle and stiff material than the other choline-based IJs. These results are related with the water content present in the jellified matrix. The IJs with elastomeric mechanic behavior had more water content than IJ – [Ch][Ib], showing its importance for the elasticity of IJ dense films.

The electrospinning of other biopolymers such as DNA and N,N – dimethylchitosan in ILs was evaluated. Despite the impossibility of fiber production from these polymers and solubilization problems, preliminary results are encouraging.

6 FUTURE WORK

This work shows for the first time the potential and effectiveness of electrospun IJ fibers to improve IL properties. In the case of IL-API, electrospun IJ fibers are an appropriate way to develop a drug delivery system.

The results of this work open up a broad range of possible future studies.

First and foremost, IJ-[Ch][Ma] should be tested in a larger variety of bacterial strains in order to determine its range of antibacterial activity.

Taking into account the fiber accumulation on the electric heater's grid during electrospinning, novel ways to keep the polymer solution in the melt state should be studied in order to improve fiber production yield. A possible approach would be a coaxial syringe heater and evaluate its effect on the whole electrospinning process, including fiber yield.

There is also evidence that the functionalization of choline-like cations in antimicrobial ILs have an important effect on antimicrobial activity. It is of interest to continue developing new antibacterial ILs and better drug delivery systems to improve their features.

For instance, another interesting future work that can be explored in the near-future is the investigation of how functionalization of choline cation in IL – [Ch][Ma] (and further IJ electrospinning) could affect its antimicrobial activity. The possibility of improving choline-cation lipophilicity in this case is highly desirable. Another approach can be the complete substitution of the choline cation for another slightly more lipophilic, with the aim of improving IL-API interaction with cellular membranes.

Taking into account the tensile tests results obtained for IJ, more studies should be made in order to truly understand not only the impact of water, but also the impact of cations and anions on the mechanical properties of IJs.

At last, another interesting challenge that should be taken is the development of a successful electrospinning process for fiber production from DNA and N,N – Dimethylchitosan in ILs. The possible results that may arise from the combination of ILs with these polymers is quite unexpected.

7 REFERENCES

1. Ohno, H., *Functional Design of Ionic Liquids.* Bulletin of the Chemical Society of Japan, 2006. **79**(11): p. 1665-1680.
2. Wilkes, J.S. and M.J. Zaworotko, *Air and water stable 1-ethyl-3-methylimidazolium based ionic liquids.* Journal of the Chemical Society, Chemical Communications, 1992(13): p. 965-967.
3. Wasserscheid, P. and W. Keim, *Ionic Liquids—New "Solutions" for Transition Metal Catalysis.* Angewandte Chemie International Edition, 2000. **39**(21): p. 3772-3789.
4. Yoshida, Y., O. Baba, and G. Saito, *Ionic Liquids Based on Dicyanamide Anion: Influence of Structural Variations in Cationic Structures on Ionic Conductivity†.* The Journal of Physical Chemistry B, 2007. **111**(18): p. 4742-4749.
5. Seddon, K.R., *Ionic Liquids for Clean Technology.* Journal of Chemical Technology & Biotechnology, 1997. **68**(4): p. 351-356.
6. Krossing, I., et al., *Why Are Ionic Liquids Liquid? A Simple Explanation Based on Lattice and Solvation Energies.* Journal of the American Chemical Society, 2006. **128**(41): p. 13427-13434.
7. Garcia, M.T., N. Gathergood, and P.J. Scammells, *Biodegradable ionic liquids : Part II. Effect of the anion and toxicology.* Green Chemistry, 2005. **7**(1): p. 9.
8. Stasiewicz, M., et al., *Assessing toxicity and biodegradation of novel, environmentally benign ionic liquids (1-alkoxymethyl-3-hydroxypyridinium chloride, saccharinate and acesulfamates) on cellular and molecular level.* Ecotoxicol Environ Saf, 2008. **71**(1): p. 157-65.
9. Choi, Y.-S., et al., *Ionic liquids as benign catalysts for the carbonylation of amines to formamides.* Applied Catalysis A: General, 2011. **404**(1-2): p. 87-92.
10. Coleman, D. and N. Gathergood, *Biodegradation studies of ionic liquids.* Chem Soc Rev, 2010. **39**(2): p. 600-37.
11. Plechkova, N.V. and K.R. Seddon, *Applications of ionic liquids in the chemical industry.* Chem Soc Rev, 2008. **37**(1): p. 123-50.
12. Erdmenger, T., et al., *Influence of different branched alkyl side chains on the properties of imidazolium-based ionic liquids.* Journal of Materials Chemistry, 2008. **18**(43): p. 5267.
13. Holbrey, J.D. and K.R. Seddon, *The phase behaviour of 1-alkyl-3-methylimidazolium tetrafluoroborates; ionic liquids and ionic liquid crystals.* Journal of the Chemical Society, Dalton Transactions, 1999(13): p. 2133-2140.
14. M. Gordon, C., et al., *Ionic liquid crystals: hexafluorophosphate salts.* Journal of Materials Chemistry, 1998. **8**(12): p. 2627-2636.
15. Huddleston, J.G., et al., *Characterization and comparison of hydrophilic and hydrophobic room temperature ionic liquids incorporating the imidazolium cation.* Green Chemistry, 2001. **3**(4): p. 156-164.
16. Marsh, K., *Room temperature ionic liquids and their mixtures—a review.* Fluid Phase Equilibria, 2004. **219**(1): p. 93-98.
17. Earle, M.J., et al., *The distillation and volatility of ionic liquids.* Nature, 2006. **439**(7078): p. 831-4.
18. Rebelo, L.P.N., et al., *On the Critical Temperature, Normal Boiling Point, and Vapor Pressure of Ionic Liquids.* The Journal of Physical Chemistry B, 2005. **109**(13): p. 6040-6043.
19. Kabo, G.J., et al., *Thermodynamic Properties of 1-Butyl-3-methylimidazolium Hexafluorophosphate in the Condensed State.* Journal of Chemical & Engineering Data, 2004. **49**(3): p. 453-461.

20. Earle, M.J. and K.R. Seddon, *Ionic liquids. Green solvents for the future.* Pure Appl. Chem., 2000. **72**(7): p. 1391-1398.
21. MacFarlane, D.R., et al., *Low viscosity ionic liquids based on organic salts of the dicyanamide anion.* Chemical Communications, 2001(16): p. 1430-1431.
22. Kölle, P. and R. Dronskowski, *Synthesis, Crystal Structures and Electrical Conductivities of the Ionic Liquid Compounds Butyldimethylimidazolium Tetrafluoroborate, Hexafluorophosphate and Hexafluoroantimonate.* European Journal of Inorganic Chemistry, 2004. **2004**(11): p. 2313-2320.
23. Stoppa, A., et al., *The Conductivity of Imidazolium-Based Ionic Liquids from (−35 to 195) °C. A. Variation of Cation's Alkyl Chain†.* Journal of Chemical & Engineering Data, 2010. **55**(5): p. 1768-1773.
24. Hagiwara, R. and Y. Ito, *Room temperature ionic liquids of alkylimidazoliumcations and fluoroanions.* Journal Fluorine Chemistry, 2000. **105**: p. 221-227.
25. Galinski, M., A. Lewandowski, and I. Stepniak, *Ionic liquids as electrolytes.* Electrochimica Acta, 2006. **51**(26): p. 5567-5580.
26. Ong, S.P., et al., *Electrochemical Windows of Room-Temperature Ionic Liquids from Molecular Dynamics and Density Functional Theory Calculations.* Chemistry of Materials, 2011. **23**(11): p. 2979-2986.
27. Suarez, P.A.Z., et al., *Enlarged electrochemical window in dialkyl-imidazolium cation based room-temperature air and water-stable molten salts.* Electrochimica Acta, 1997. **42**(16): p. 2533-2535.
28. Welton, T., *Room-Temperature Ionic Liquids. Solvents for Synthesis and Catalysis.* Chem. Rev., 1999. **99**: p. 2071.
29. Hallett, J.P. and T. Welton, *Room-temperature ionic liquids: solvents for synthesis and catalysis. 2.* Chem Rev, 2011. **111**(5): p. 3508-76.
30. Swatloski, R.P., et al., *Dissolution of Cellose with Ionic Liquids.* Journal of the American Chemical Society, 2002. **124**(18): p. 4974-4975.
31. Wang, W.-T., et al., *Dissolution Behavior of Chitin in Ionic Liquids.* Journal of Macromolecular Science, Part B, 2010. **49**(3): p. 528-541.
32. Rantwijk, F.v. and R.A. Sheldon, *Biocatalysis in Ionic Liquids.* Chem. Rev., 2007. **107**: p. 2757-2785.
33. Dominguez de Maria, P. and Z. Maugeri, *Ionic liquids in biotransformations: from proof-of-concept to emerging deep-eutectic-solvents.* Curr Opin Chem Biol, 2011. **15**(2): p. 220-5.
34. Burba, C.M., et al., *Cation−Anion Interactions in 1-Ethyl-3-Methylimidazolium Trifluoromethanesulfonate-Based Ionic Liquid Electrolytes.* The Journal of Physical Chemistry B, 2008. **112**(10): p. 2991-2995.
35. Xu, K., *Nonaqueous Liquid Electrolytes for Lithium-Based Rechargeable Batteries.* Chem Rev, 2004. **104**(10): p. 4303-4418.
36. Shin, J., *Ionic liquids to the rescue? Overcoming the ionic conductivity limitations of polymer electrolytes.* Electrochemistry Communications, 2003. **5**(12): p. 1016-1020.
37. de Souza, R.F., et al., *Room temperature dialkylimidazolium ionic liquid-based fuel cells.* Electrochemistry Communications, 2003. **5**(8): p. 728-731.
38. Izawa, H. and J.-i. Kadokawa, *Preparation and characterizations of functional ionic liquid-gel and hydrogel materials of xanthan gum.* Journal of Materials Chemistry, 2010. **20**(25): p. 5235.
39. Torimoto, T., et al., *New Frontiers in Materials Science Opened by Ionic Liquids.* Advanced Materials, 2010. **22**(11): p. 1196-1221.
40. Vidinha, P., et al., *Ion jelly: a tailor-made conducting material for smart electrochemical devices.* Chem Commun (Camb), 2008(44): p. 5842-4.

41. Lourenço, N.M.T., et al., *Effect of gelatin–ionic liquid functional polymers on glucose oxidase and horseradish peroxidase kinetics.* Reactive and Functional Polymers, 2011. **71**(4): p. 489-495.
42. Buhler, G. and C. Feldmann, *Microwave-assisted synthesis of luminescent LaPO4:Ce,Tb nanocrystals in ionic liquids.* Angew Chem Int Ed Engl, 2006. **45**(29): p. 4864-7.
43. Weng, L., et al., *Effect of tetraalkylphosphonium based ionic liquids as lubricants on the tribological performance of a steel-on-steel system.* Tribology Letters, 2006. **26**(1): p. 11-17.
44. Luis, P., et al., *Facilitated transport of CO2 and SO2 through Supported Ionic Liquid Membranes (SILMs).* Desalination, 2009. **245**(1-3): p. 485-493.
45. Soukup-Hein, R.J., M.M. Warnke, and D.W. Armstrong, *Ionic liquids in analytical chemistry.* Annu Rev Anal Chem (Palo Alto Calif), 2009. **2**: p. 145-68.
46. Hayashi, S., S. Saha, and H. Hamaguchi, *A new class of magnetic fluids: bmim[FeCl4] and nbmim[FeCl4] ionic liquids.* Magnetics, IEEE Transactions on, 2006. **42**(1): p. 12-14.
47. Courthéoux, L., et al., *Facile Catalytic Decomposition at Low Temperature of Energetic Ionic Liquid as Hydrazine Substitute.* European Journal of Inorganic Chemistry, 2005. **2005**(12): p. 2293-2295.
48. Lunstroot, K., et al., *Luminescent Ionogels Based on Europium-Doped Ionic Liquids Confined within Silica-Derived Networks.* Chemistry of Materials, 2006. **18**(24): p. 5711-5715.
49. Noble, R.D. and D.L. Gin, *Perspective on ionic liquids and ionic liquid membranes.* Journal of Membrane Science, 2011. **369**(1-2): p. 1-4.
50. Wu, B., R.G. Reddy, and R.D. Rogers, *Novel ionic liquid thermal storage for solar thermal electric power systems.* Proceedings of Solar Forum 2001 Solar Energy: The Power to Choose April 21-25, 2001, Washington, DC, 2001: p. 445-451.
51. Tempel, D.J., et al., *High Gas Storage Capacities for Ionic Liquids through Chemical Complexation.* Journal of the American Chemical Society, 2007. **130**(2): p. 400-401.
52. Adler, R. *Reports on Science and Technology*. Wiesbaden 2006 17-08-2011]; Available from: http://www.the-linde-group.com/en/images/Linde_Technology_1_2006_EN14-10188.pdf.
53. BASF. *BASIL™– The first commercial process using ionic liquids*. 2004 17-08-2011]; Available from: http://www.basf.com/group/corporate/en/innovations/innovation-award/2004/basil.
54. Hough, W.L., et al., *The third evolution of ionic liquids: active pharmaceutical ingredients.* New Journal of Chemistry, 2007. **31**(8): p. 1429.
55. Wood, N. and G. Stephens, *Accelerating the discovery of biocompatible ionic liquids.* Physical Chemistry Chemical Physics, 2010. **12**(8): p. 1670-1674.
56. Wells, A.S. and V.T. Coombe, *On the Freshwater Ecotoxicity and Biodegradation Properties of Some Common Ionic Liquids.* Organic Process Research & Development, 2006. **10**(4): p. 794-798.
57. Matzke, M., et al., *The influence of anion species on the toxicity of 1-alkyl-3-methylimidazolium ionic liquids observed in an (eco)toxicological test battery.* Green Chemistry, 2007. **9**(11): p. 1198.
58. Higdon, J. *Micronutrient Information Center - Choline*. 2008 01-12-2011]; Available from: http://lpi.oregonstate.edu/infocenter/othernuts/choline/.
59. Duan, Z., Y. Gu, and Y. Deng, *Green and moisture-stable Lewis acidic ionic liquids (choline chloride · xZnCl2) catalyzed protection of carbonyls at room temperature under solvent-free conditions.* Catalysis Communications, 2006. **7**(9): p. 651-656.
60. Vijayaraghavan, R., et al., *Biocompatibility of choline salts as crosslinking agents for collagen based biomaterials.* Chemical Communications, 2010. **46**(2): p. 294-296.

61. Vrikkis, R.M., et al., *Biocompatible Ionic Liquids: A New Approach for Stabilizing Proteins in Liquid Formulation.* Journal of Biomechanical Engineering, 2009. **131**(7): p. 074514-4.
62. Mevellec, V., et al., *Organic phase stabilization of rhodium nanoparticle catalyst by direct phase transfer from aqueous solution to room temperature ionic liquid based on surfactant counter anion exchange.* Chemical Communications, 2005(22): p. 2838-2839.
63. Kawai, K., et al., *Bioinspired Choline-like Ionic Liquids: Their Penetration Ability through Cell Membranes and Application to SEM Visualization of Hydrous Samples.* Langmuir, 2011. **27**(16): p. 9671-9675.
64. Pernak, J. and P. Chwała, *Synthesis and anti-microbial activities of choline-like quaternary ammonium chlorides.* European Journal of Medicinal Chemistry, 2003. **38**(11-12): p. 1035-1042.
65. Pernak, J., et al., *Choline-derivative-based ionic liquids.* Chemistry, 2007. **13**(24): p. 6817-27.
66. Stoimenovski, J., et al., *Crystalline vs. ionic liquid salt forms of active pharmaceutical ingredients: a position paper.* Pharm Res, 2010. **27**(4): p. 521-6.
67. Karpinski, P.H., *Polymorphism of Active Pharmaceutical Ingredients.* Chemical Engineering & Technology, 2006. **29**(2): p. 233-237.
68. Vippagunta, S.R., H.G. Brittain, and D.J.W. Grant, *Crystalline solids.* Advanced Drug Delivery Reviews, 2001. **48**(1): p. 3-26.
69. Bauer, J., et al., *Ritonavir: An Extraordinary Example of Conformational Polymorphism.* Pharm Res, 2001. **18**(6): p. 859-866.
70. Raw, A.S., et al., *Regulatory considerations of pharmaceutical solid polymorphism in Abbreviated New Drug Applications (ANDAs).* Adv Drug Deliv Rev, 2004. **56**(3): p. 397-414.
71. Hörter, D. and J.B. Dressman, *Influence of physicochemical properties on dissolution of drugs in the gastrointestinal tract.* Advanced Drug Delivery Reviews, 2001. **46**(1-3): p. 75-87.
72. Ferraz, R., et al., *Ionic liquids as active pharmaceutical ingredients.* ChemMedChem, 2011. **6**(6): p. 975-85.
73. Hough-Troutman, W.L., et al., *Ionic liquids with dual biological function: sweet and anti-microbial, hydrophobic quaternary ammonium-based salts.* New Journal of Chemistry, 2009. **33**(1): p. 26.
74. Demberelnyamba, D., et al., *Synthesis and antimicrobial properties of imidazolium and pyrrolidinonium salts.* Bioorg Med Chem, 2004. **12**(5): p. 853-7.
75. Carson, L., et al., *Antibiofilm activities of 1-alkyl-3-methylimidazolium chloride ionic liquids.* Green Chemistry, 2009. **11**(4): p. 492.
76. Saadeh, S.M., et al., *New room temperature ionic liquids with interesting ecotoxicological and antimicrobial properties.* Ecotoxicol Environ Saf, 2009. **72**(6): p. 1805-9.
77. Pernak, J. and J. Feder-Kubis, *Synthesis and properties of chiral ammonium-based ionic liquids.* Chemistry, 2005. **11**(15): p. 4441-9.
78. Pernak, J., et al., *Synthesis and properties of chiral imidazolium ionic liquids with a (1R,2S,5R)-(?)-menthoxymethyl substituent.* New Journal of Chemistry, 2007. **31**(6): p. 879.
79. Docherty, K.M. and J.C.F. Kulpa, *Toxicity and antimicrobial activity of imidazolium and pyridinium ionic liquids.* Green Chemistry, 2005. **7**(4): p. 185.
80. Walkiewicz, F., et al., *Multifunctional long-alkyl-chain quaternary ammonium azolate based ionic liquids.* New Journal of Chemistry, 2010. **34**(10): p. 2281.
81. Pernak, J., I. Goc, and I. Mirska, *Anti-microbial activities of protic ionic liquids with lactate anion.* Green Chemistry, 2004. **6**(7): p. 323.

82. Pernak, J., K. Sobaszkiewicz, and J. Foksowicz-Flaczyk, *Ionic liquids with symmetrical dialkoxymethyl-substituted imidazolium cations.* Chemistry, 2004. **10**(14): p. 3479-85.
83. Pernak, J., K. Sobaszkiewicz, and I. Mirska, *Anti-microbial activities of ionic liquids.* Green Chemistry, 2003. **5**(1): p. 52-56.
84. Bernot, R.J., E.E. Kennedy, and G.A. Lamberti, *Effects of ionic liquids on the survival, movement, and feeding behavior of the freshwater snail, Physa acuta.* Environmental Toxicology and Chemistry, 2005. **24**(7): p. 1759-1765.
85. Stock, F., et al., *Effects of ionic liquids on the acetylcholinesterase - a structure - activity relationship consideration.* Green Chemistry, 2004. **6**(6): p. 286.
86. Kono, K. and K. Arakawa, *Methicillin-resistant Staphylococcus aureus (MRSA) isolated in clinics and hospitals in the Fukuoka city area.* Journal of Hospital Infection, 1995. **29**(4): p. 265-273.
87. Romanelli, R.M.C., et al., *MRSA outbreak at a transplantation unit.* The Brazilian Journal of Infectious Diseases. **14**(1): p. 54-59.
88. Kumar, V. and S.V. Malhotra, *Study on the potential anti-cancer activity of phosphonium and ammonium-based ionic liquids.* Bioorg Med Chem Lett, 2009. **19**(16): p. 4643-6.
89. Goho, A., *Tricky business: The crystal form of a drug can be the secret to its success.* Science News, 2004. **166**(8): p. 122-124.
90. Hough, W.L. and R.D. Rogers, *Ionic Liquids Then and Now: From Solvents to Materials to Active Pharmaceutical Ingredients.* Bulletin of the Chemical Society of Japan, 2007. **80**(12): p. 2262-2269.
91. Bica, K., et al., *In search of pure liquid salt forms of aspirin: ionic liquid approaches with acetylsalicylic acid and salicylic acid.* Phys Chem Chem Phys, 2010. **12**(8): p. 2011-7.
92. Kumar, V. and S.V. Malhotra, *Ionic Liquids as Pharmaceutical Salts: A Historical Perspective.* 2010. **1038**: p. 1-12.
93. Hu, H., et al., *Immobilization of Ionic Liquids in Layered Compounds via Mechanochemical Intercalation.* The Journal of Physical Chemistry C, 2011. **115**(13): p. 5509-5514.
94. Gao, H., et al., *Immobilization of Ionic Liquid [BMIM][PF6] by Spraying Suspension Dispersion Method.* Industrial & Engineering Chemistry Research, 2008. **47**(13): p. 4414-4417.
95. Mehnert, C.P., *Supported ionic liquid catalysis.* Chemistry, 2004. **11**(1): p. 50-6.
96. Sugimura, R., et al., *Immobilization of acidic ionic liquids by copolymerization with styrene and their catalytic use for acetal formation.* Catalysis Communications, 2007. **8**(5): p. 770-772.
97. Bellayer, S., et al., *Immobilization of ionic liquids in translucent tin dioxide monoliths by sol–gel processing.* Dalton Transactions, 2009(8): p. 1307.
98. Lu, W., et al., *Use of ionic liquids for pi-conjugated polymer electrochemical devices.* Science, 2002. **297**(5583): p. 983-7.
99. Le Bideau, J., L. Viau, and A. Vioux, *Ionogels, ionic liquid based hybrid materials.* Chem Soc Rev, 2011. **40**(2): p. 907-25.
100. Gorlov, M. and L. Kloo, *Ionic liquid electrolytes for dye-sensitized solar cells.* Dalton Trans, 2008(20): p. 2655-66.
101. Terasawa, N., et al., *High performance polymer actuator based on carbon nanotube-ionic liquid gel: Effect of ionic liquid.* Sensors and Actuators B: Chemical, 2011. **156**(2): p. 539-545.
102. Park, J.H., et al., *Targeted delivery of low molecular drugs using chitosan and its derivatives.* Adv Drug Deliv Rev, 2010. **62**(1): p. 28-41.
103. Cao, H., et al., *RNA interference by nanofiber-based siRNA delivery system.* Journal of Controlled Release, 2010. **144**(2): p. 203-212.

104. Puppi, D., et al., *Poly(lactic-co-glycolic acid) electrospun fibrous meshes for the controlled release of retinoic acid.* Acta Biomaterialia, 2010. **6**(4): p. 1258-1268.
105. Torchilin, V., *Antibody-modified liposomes for cancer chemotherapy.* Expert Opinion on Drug Delivery, 2008. **5**(9): p. 1003-1025.
106. Sampathkumar, S.-G. and K.J. Yarema, *Targeting Cancer Cells with Dendrimers.* Chemistry & Biology, 2005. **12**(1): p. 5-6.
107. Viau, L., et al., *Ionogels as drug delivery system: one-step sol-gel synthesis using imidazolium ibuprofenate ionic liquid.* Chemical Communications, 2010. **46**(2): p. 228-230.
108. Trewyn, B.G., C.M. Whitman, and V.S.Y. Lin, *Morphological Control of Room-Temperature Ionic Liquid Templated Mesoporous Silica Nanoparticles for Controlled Release of Antibacterial Agents.* Nano Letters, 2004. **4**(11): p. 2139-2143.
109. Zhang, Y., et al., *Synthesis and Biological Applications of Imidazolium-Based Polymerized Ionic Liquid as a Gene Delivery Vector.* Chemical Biology & Drug Design, 2009. **74**(3): p. 282-288.
110. Langer, R. and D.A. Tirrell, *Designing materials for biology and medicine.* Nature, 2004. **428**(6982): p. 487-492.
111. Nair, L.S. and C.T. Laurencin, *Polymers as Biomaterials for Tissue Engineering and Controlled Drug Delivery.* 2006. **102**: p. 47-90.
112. Sill, T.J. and H.A. von Recum, *Electrospinning: Applications in drug delivery and tissue engineering.* Biomaterials, 2008. **29**(13): p. 1989-2006.
113. Schiffman, J.D. and C.L. Schauer, *A Review: Electrospinning of Biopolymer Nanofibers and their Applications.* Polymer Reviews, 2008. **48**(2): p. 317-352.
114. He, J.-H., Y.-Q. Wan, and L. Xu, *Nano-effects, quantum-like properties in electrospun nanofibers.* Chaos, Solitons & Fractals, 2007. **33**(1): p. 26-37.
115. Huang, Z.-M., et al., *Electrospinning and mechanical characterization of gelatin nanofibers.* Polymer, 2004. **45**(15): p. 5361-5368.
116. Viswanathan, G., et al., *Preparation of Biopolymer Fibers by Electrospinning from Room Temperature Ionic Liquids.* Biomacromolecules, 2006. **7**(2): p. 415-418.
117. Ki, C.S., et al., *Characterization of gelatin nanofiber prepared from gelatin–formic acid solution.* Polymer, 2005. **46**(14): p. 5094-5102.
118. Zhang, S., et al., *Gelatin nanofibrous membrane fabricated by electrospinning of aqueous gelatin solution for guided tissue regeneration.* J Biomed Mater Res A, 2009. **90**(3): p. 671-9.
119. Pimenta, A.F.R., et al., *Electrospinning of Ion Jelly fibers.* Submitted to Acta Materiala, 2011.
120. Skoog, D.A., F.J. Holler, and S.R. Crouch, *Principles of Instrumental Analysis 6th ed*2006: Brooks Cole.
121. Czichos, H., T. Saito, and L. Smith, *Springer handbook of materials measurement methods*2006: Springer.
122. Miller, J.H., *Experiments in Molecular Genetics*1972: Cold Spring harbor Laboratory Pr.
123. Bigi, A., et al., *Mechanical and thermal properties of gelatin films at different degrees of glutaraldehyde crosslinking.* Biomaterials, 2001. **22**(8): p. 763-768.
124. Carvalho, T., et al., *Understanding the Ion-Jelly conductivity mechanism.* Submitted, 2011.
125. Arumugam, G.K., S. Khan, and P.A. Heiden, *Comparison of the Effects of an Ionic Liquid and Other Salts on the Properties of Electrospun Fibers, 2 - Poly(vinyl alcohol).* Macromolecular Materials and Engineering, 2009. **294**(1): p. 45-53.
126. Seo, J.M., et al., *Comparison of the Effects of an Ionic Liquid and Triethylbenzylammonium Chloride on the Properties of Electrospun Fibers, 1 - Poly(lactic acid).* Macromolecular Materials and Engineering, 2009. **294**(1): p. 35-44.

127. Sung, J., et al., *Air–liquid interface of ionic liquid + H2O binary system studied by surface tension measurement and sum-frequency generation spectroscopy.* Chemical Physics Letters, 2005. **406**(4-6): p. 495-500.
128. Taylor, M.B., *Summary of Mandelic Acid for the Improvement of Skin Conditions*, in *Cosmetic Dermatology*1999. p. 26-28.
129. van Putten, P.L., *Mandelic acid and urinary tract infections.* Antoine van Leeuwenhoek, 1979. **45**.
130. Gordon, T., et al., *Synthesis and characterization of zinc/iron oxide composite nanoparticles and their antibacterial properties.* Colloids and Surfaces A: Physicochemical and Engineering Aspects, 2011. **374**(1-3): p. 1-8.
131. Adams, S.S., et al., *Absorption, distribution and toxicity of ibuprofen.* Toxicology and Applied Pharmacology, 1969. **15**(2): p. 310-330.
132. Groover, M.P., *Fundamentals of Modern Manufacturing: Materials, Processes, and Systems 4th Ed.*2010: John Wiley and Sons.
133. Treolar, L.R.G., *The physics of rubber elasticity*2005: Oxford University Press

134. Fang, X. and D.H. Reneker, *DNA fibers by electrospinning.* Journal of Macromolecular Science, Part B, 1997. **36**(2): p. 169-173.
135. Takahashi, T., M. Taniguchi, and T. Kawai, *Fabrication of DNA Nanofibers on a Planar Surface by Electrospinning.* Jpn. J. Appl. Phys., 2005. **44**(27): p. 860-862.
136. Liu, Y., et al., *Preparation of novel ultrafine fibers based on DNA and poly(ethylene oxide) by electrospinning from aqueous solutions.* Reactive and Functional Polymers, 2007. **67**(5): p. 461-467.
137. Tanaka, K. and Y. Okahata, *A DNA−Lipid Complex in Organic Media and Formation of an Aligned Cast Film1.* Journal of the American Chemical Society, 1996. **118**(44): p. 10679-10683.
138. Rabea, E.I., et al., *Chitosan as Antimicrobial Agent: Applications and Mode of Action.* Biomacromolecules, 2003. **4**(6): p. 1457-1465.